Agricultural Water Management 279 (2023) 108209

Contents lists available at ScienceDirect

Agricultural Water Management

journal homepage: www.elsevier.com/locate/agwat

Water use and soil water balance of Mediterranean tree crops assessed with the SIMDualKc model in orchards of southern Portugal

Tiago B. Ramos [a,*], Hanaa Darouich [b], Ana R. Oliveira [a], Mohammad Farzamian [c], Tomás Monteiro [d], Nádia Castanheira [c], Ana Paz [c], Maria C. Gonçalves [c], Luís S. Pereira [b]

[a] Centro de Ciência e Tecnologia do Ambiente e do Mar (MARETEC–LARSyS), Instituto Superior Técnico, Universidade de Lisboa, Av. Rovisco Pais, 1, 1049-001 Lisboa, Portugal
[b] LEAF—Linking Landscape, Environment, Agriculture and Food Research Center, Associated Laboratory TERRA, Instituto Superior de Agronomia, Universidade de Lisboa, Tapada da Ajuda, 1349-017 Lisboa, Portugal
[c] Instituto Nacional de Investigação Agrária e Veterinária, Avenida da República, Quinta do Marquês, 2780-157 Oeiras, Portugal
[d] Universidade de Évora, Largo dos Colegiais, N° 2, 7004–516 Évora, Portugal

ARTICLE INFO

Handling Editor - J.E. Fernández

Keywords:
Crop coefficients
Crop evapotranspiration
Dual-K_c approach
Orchards
Almond, olive, citrus, and pomegranate

ABSTRACT

Orchards consist of complex agricultural systems, with a variety of characteristics (planting density, tree height, training system, canopy cover, irrigation method, interrow management) influencing crop evapotranspiration (ET_c). Thus, irrigation water management requires finding crop coefficients (K_c) that represent the characteristics of local orchards, evidencing the need for site specific data. The main objective of this study was to derive the K_c of almond, olive, citrus, and pomegranate orchards in Alentejo, southern Portugal, wherein they became dominant over the last decade. Monitoring was carried out in nine orchards, which management decisions were performed by the farmers. The ET_c was estimated from the soil water balance computed for each orchard using the FAO56 dual-K_c approach with the SIMDualKc model. The model successfully simulated the soil water contents measured in the various fields along two growing seasons, with root mean square error values lower than 0.005 $m^3\ m^{-3}$ and modeling efficiencies from 0.363 to 0.782. The estimated basal crop coefficients (K_{cb}) for the initial, mid- and end-seasons were respectively 0.22, 0.58, and 0.50 for almond; 0.32–0.33, 0.35–0.36, and 0.33–0.34 for olive; 0.40, 0.40–41, and 0.40–0.41 for citrus; and 0.24, 0.60, and 0.52 for pomegranate. Small variations in olive and citrus K_{cb} values were found to be related to differences in the fraction of the ground covered by trees' canopies and tree height. The single K_c values, which included the component relative to soil evaporation, were also estimated. Furthermore, evaluation of the soil water balance in the nine case studies showed salinity effects in one almond orchard, mild irrigation water deficits in olive systems, and large non-consumptive water use in citrus and pomegranate orchards. These results evidence the need for better management of orchards irrigation water in the region, and the current study provides for reliable information on the K_c of tree crops to support improving the management of local orchard systems and the preservation of soil and water resources. Aimed at these resources and the sustainability of their use, simulated alternative irrigation schedules were performed, which identified possible water savings of 20 mm in case of olives, up to 855 mm for citrus.

1. Introduction

The expansion of the irrigated area over the past century has provided the means for agricultural production in regions of the world where scarcity prevails. In these regions mostly afflicted by arid, semi-arid, and dry sub-humid climates, irrigation is fundamental to fulfill crop water requirements, diversify crop production, increase food production, meet the growing food demand, ensure food stability, and increase the prosperity of rural areas (Pereira et al., 2009). This, most times, comes with costs to the environment as the pressure on freshwater resources builds up. Irrigation is today responsible for 70% of all freshwater withdrawals in the world and 90% in the least developed regions (UNESCO, 2020). Irrigation is also considered a key source of land degradation, namely by contributing to the contamination or

* Correspondence to: MARETEC–LARSyS, Instituto Superior Técnico, Av. Rovisco Pais, 1049-001 Lisbon, Portugal.
E-mail addresses: tiago_ramos@netcabo.pt, tiagobramos@tecnico.ulisboa.pt (T.B. Ramos).

https://doi.org/10.1016/j.agwat.2023.108209
Received 10 October 2022; Received in revised form 29 January 2023; Accepted 31 January 2023
Available online 6 February 2023
0378-3774/© 2023 The Authors. Published by Elsevier B.V. This is an open access article under the CC BY-NC-ND license (http://creativecommons.org/licenses/by-nc-nd/4.0/).

depletion of water resources, promotion of soil erosion and soil salinization, being also associated with biodiversity loss. Climate change only further exacerbates the scarcity issue and future uncertainty.

Mitigating the environmental problems referred to above as well as climate uncertainty can only be achieved by improving agricultural water management, namely water use and performance of irrigation systems (Pereira et al., 2002; Jovanovic et al., 2020). This requires an accurate estimate of crop water requirements and irrigation schedules (irrigation timing, duration, and quantity), namely by following the FAO56 method (Allen et al., 1998). Widely used, this method estimates crop evapotranspiration (ET_c) as the product of a crop coefficient (K_c) and the grass reference evapotranspiration (ET_o), the latter being calculated with the FAO Penman–Monteith (FAO-PM) equation (Allen et al., 1998). K_c values are defined for each crop stage by using the single crop coefficient approach, which assumes a single value for including both the soil evaporation and crop transpiration processes, or the dual crop coefficient approach ($K_c = K_{cb} + K_e$), which separately considers the basal transpiration coefficient (K_{cb}) and the soil evaporation coefficient (K_e). The methodology is straightforward, with standard K_c and K_{cb} values available for most field and vegetable crops (Pereira et al., 2021a, 2021b). For trees and vines, Rallo et al. (2021) also provided standard K_c values for the most common agricultural species and management options. However, the complexity of orchard systems is great because surfaces are heterogenous and the soil is incompletely covered, and differences in the planting density, canopy height, training system, interrow management, and irrigation method influence the amount of energy available for both the transpiration and soil evaporation processes. It results that the collected literature information may be rather insufficient for selecting from the reported K_c and K_{cb} values for those to be efficiently used in irrigation water management (Rallo et al., 2021; Pereira et al., 2020a; Volschenk, 2020; Fereres et al., 2012).

That knowledge gap is particularly relevant for the Alentejo region of southern Portugal, where orchards systems have become dominant over the last decade. The implementation of the Alqueva project in 2002, which progressively added 120,000 ha of newly irrigated land to the already existing 35,000 ha included in different collective systems, provided conditions for the fast expansion of olive orchards and other perennial crops (Ramos et al., 2019). Olive (87,500 ha) and other orchards (22,000 ha) (DGADR, 2021), from which almond stands out, now extend throughout the landscape, replacing the traditional crops, mainly irrigated and rainfed cereals. In the Alqueva irrigation district alone, olives and almonds cover today 56.7% and 21.3% of the equipped area, respectively (EDIA, 2022). These orchards mostly consist of high (≥300 trees ha^{-1}) and very high-density (≥1500 trees ha^{-1}) orchard systems, which require high to very-high input factors (Paço et al., 2019).

The abrupt landscape change has naturally raised doubts about the sustainability of the new production systems, with local populations often raising concerns about respective environmental impacts as often reported by the traditional and social media (Expresso, 2018; Dinheiro Vivo, 2021; Publico, 2021). This social unrest is per se pressing on the viability of those systems, resulting in the need for a throughout and clear quantification of the main environmental risks associated with the new cropping reality in the Alentejo region. While some studies already exist to address improved crop water use (Paço et al., 2019, 2014; Santos, 2018; Conceição et al., 2017), and decrease soil salinization risks (Ramos et al., 2019) and non-point source pollution due to fertigation practices (Cameira et al., 2014), these studies imply further assessing crop water use to better control environmental impacts. Meanwhile, studies are limited to olive and are insufficient to provide guidelines for improving irrigation and fertigation practices to local farmers.

The current study follows the need to increase knowledge on the water use and environmental impacts of the new orchard systems dominating the landscape in the Alentejo region, southern Portugal. The first part of the study aims to assess local irrigation practices through the accurate estimate of evapotranspiration and crop coefficients in different orchards systems. The selected tool was the SIMDualKc model (Rosa et al., 2012), which adopts the FAO-56 dual-K_c approach for computing ET_c fluxes when partitioning into crop transpiration and soil evaporation. A review on water balance models justifies that option (Pereira et al., 2020b). The reasons for choosing this model further lay on: (i) the acknowledged more accurate estimates of the evapotranspiration processes provided by the FAO-56 dual-K_c approach as compared to other methods (Pereira et al., 2015a; Kool et al., 2014; López-Urrea et al., 2009); (ii) the adequacy in adopting the estimated potential transpiration and soil evaporation fluxes, thus defining atmospheric boundary conditions in mechanistic vadose zone modeling aimed at evaluating soil salinization and fertigation risks (Chen et al., 2022; Phogat et al., 2017; González et al., 2015; Ramos et al., 2012; Minhas et al., 2020); and (iii) the extensive testing already performed with the SIMDualKc model in orchards grown under diverse management options and climate conditions, namely for olive (Puig-Sirera et al., 2021; Paço et al., 2019, 2014), peach (Paço et al., 2012), grapevine (Darouich et al., 2022a; Silva et al., 2021; Cancela et al., 2015; Fandiño et al., 2012), and citrus (Darouich et al., 2022b).

The objectives of this study, therefore, consist of: (i) to calibrate and validate the SIMDualKc model in various almond, olive, citrus (orange, clementine, and mandarin), and pomegranate orchards of Alentejo using field data of the 2019 and 2020 growing seasons; (ii) with support by the model, to derive the K_c and K_{cb} standard and actual crop coefficients for those crops using the dual-K_c approach; (iii) to evaluate the components of the soil water balance from a water saving perspective; and, (iv) using the model, to develop alternative water saving irrigation schedules and management issues. Results of this study will also be used as input to mechanistic models aimed at predicting soil salinization and crop fertigation risks, which assessment shall be the object of companion papers to be published later. As such, this study aims to contribute to improve irrigation water use in the Alentejo region considering the sustainability and response to climate change of local production systems. A few novelties must be referred: the adoption of a dual-K_c model to assess the irrigation and related water balance of six different crops and nine fields; the gain of further data on standard basal crop coefficients for Mediterranean tree crops, which is still very limited; the use, for the first time, of a dual-K_c model for almond, mandarin, and pomegranate orchards; and not limiting the assessment to discussions on possible issues, but proposing quantified predictions of water saving for all nine plots through model simulations considering mild deficit irrigation for the crop stages when the crop and yields are not affected.

2. Material and methods

2.1. Description of the study area

This study was conducted in the Roxo irrigation district (RID), Montes Velhos, Aljustrel, Portugal, from January 1st, 2019, to December 31st, 2020. The RID is a collective system with 5041 ha, built during stage I of the irrigation plan for Alentejo, in 1968. Since 2016, the RID is connected to the Alqueva system, which provides an extra water supply during drier seasons. The climate in the region is semi-arid. The mean annual air temperature is 16.3ºC, ranging from a minimum of 9.8ºC in January to a maximum of 23.1ºC in August. The mean annual precipitation is 454 mm, which occurs mostly between October and May. The mean annual reference evapotranspiration (ET_o) computed with the FAO-PM equation (Allen et al., 1998) is 1363 mm for the period 1979–2020 (Hersbach et al., 2018). The main soil units are classified as Luvisols (~40%), Fluvisols and Regosols (~20%), Gleysols and Planosols (~20%), and Vertisols (~10%) (IUSS Working Group WRB, 2014). Soil salinization problems have long been reported in the region (Alexandre et al., 2018; Martins et al., 2005), resulting from the use of poor-quality soil drainage and irrigation water prior to the connection of the RID to the Alqueva system. Salinization may have also been aggravated due to less percolating water resulting from a decreasing precipitation trend as reported by Portela et al. (2020).

In 2019, the dominant land uses were rainfed cereals (~46%), sunflower (~14%), olive (~21%), almond (~5%), and maize (~4%). This distribution was explained by drought conditions which limited irrigation in that season. Nonetheless, olive and almond areas have been expanding despite drought conditions observed over the last decade. Drip is the most common irrigation method, but sprinkler and surface methods are also used, the latter in farms of smaller dimensions. The groundwater table depth averaged 5.5 m, with maximum and minimum depths of 7.6 and 4.2 m, respectively (SNIRH, 2022).

2.2. Experimental plots and measurements

Irrigation practices were monitored in nine commercial orchards located in the RID (Fig. 1). The selected crops were almond (*Prunus amygdalus* Batsch), olive (*Olea europaea* L.), citrus (*Citrus* spp.), and pomegranate (*Punica granatum* L.), covering the most representative perennials grown in the region. Table 1 presents the main characteristics of the selected orchards, including location, plant variety, crop density and age, training system, and soil type. In five locations, orchards were on ridges, mostly trapezoidal shaped with 0.25–0.70 m height, and 1.2–1.6 m wide at the top and 2.3–2.8 m wide at the bottom.

Table 2 gives the main physical and chemical properties of soils in the nine study sites. The soil classification follows the IUSS Working Group (2014). The particle size distribution was determined following the International Soil Science Society (ISSS) particle limits (Atterberg scale), with particles of diameter < 0.002 mm (clay) and 0.02–0.002 mm (silt) obtained using the pipette method, and particles 0.2–0.02 mm (fine sand) and 2–0.2 mm (coarse sand) obtained through sieving. The organic matter (OM, %) content was estimated from the organic carbon (OC, %) content determined by the Walkley–Black method, using the relation OM = 1.724 × OC (Nelson and Sommers, 1982). Dry bulk density (ρ_b) was determined by drying volumetric soil samples (100 cm^3) at 105ºC for 48 h. Soil hydraulic properties were measured also in 100 cm^3 undisturbed soil cores. The soil water content at saturation (θ_S) was determined from the maximum holding capacity of the soil cores on a volumetric basis. The soil water content at field capacity (θ_{FC}) was measured using suction tables at − 10 kPa matric potential (Romano et al., 2002). The soil water content at the wilting point (θ_{WP}) was measured with a pressure plate extractor at − 1500 kPa matric potential (Dane and Hopmans, 2002). Measured depths were assumed representative of the entire root zone layer, including with ridges. The electrical conductivity of the soil saturation paste extract (EC_e) was determined potentiometrically.

Meteorological data for the study period were collected at the local weather station. Data included daily values of maximum and minimum air temperatures (T_{min} and T_{max}, ºC), minimum and maximum relative humidity (RH_{min}, RH_{max}, %), solar radiation (R_s, MJ m^{-2} day^{-1}), wind speed measured at 2 m height (u_2, m s^{-1}), and rainfall (P, mm). Fig. 2 briefly characterizes the weather conditions during the study period, showing relatively similar interannual variability for most variables except for rainfall.

At every site, drip irrigation systems were used, with management practices performed according to standard practices in the region and decided by farmers, i.e., applying daily small irrigation depths. Drippers were spaced 0.7–1.0 m apart, placed under tree canopies in a single line in almond and olive plots and two lines in citrus and pomegranate plots. Table 3 shows the main characteristics of irrigation events, namely initiation and end dates, depths per event, the fraction of the soil surface wetted by irrigation (f_w), and the total seasonal application depths. Irrigation depths per irrigation event averaged between 2.7 (P6) and 7.4 mm (P8). The season irrigation depths per cropped fields averaged 658 mm in almond, 320 mm in olive, 830 mm in citrus, and 791 mm in pomegranate. Depths were monitored using a flowmeter inserted in the drip lines. Irrigation was carried out nearly every day during the summer dry season and less frequently during spring and autumn.

Soil water contents were continuously monitored at depths of 0.1, 0.3, 0.5, and 0.7 m using EnviroPro MT capacitance probes (MAIT Industries, Australia). Probes were installed in the crop rows, with varying distances from emitters but always less than 0.3 m. Fig. 3 presents, as an example, the monitoring area in P1, showing the relative positions of the

Fig. 1. Location of the study area.

Table 1
Location and general characteristics of the case studies.

Field plot	Crop	Variety	Latitude	Longitude	Density (trees ha^{-1})	Age	Training system	Soil *	Slope (%)	Ridges
P1	Almond	Monterey	37.9387	-8.1525	391	5	Vase	Chromic Abruptic Luvisol	5.0	No
P2	Almond	Monterey	37.9407	-8.1536	391	5	Vase	Chromic Abruptic Luvisol	5.0	No
P3	Olive	Arbequina	37.9407	-8.1419	319	11	Vase	Chromic Dystric Cambisol	< 1.0	Yes
P4	Olive	Cobrançosa	37.9512	-8.1538	297	12	Vase	Chromic Dystric Cambisol	< 1.0	No
P5	Olive	Picual	37.9540	-8.1398	297	11	Vase	Calcaric Regosol	1.0 – 2.0	No
P6	Orange	Fukumoto	37.9700	-8.1808	404	5	Vase	Chromic Abruptic Luvisol	1.0 – 2.0	Yes
P7	Clementine	Oronules	37.9697	-8.1758	675	5	Vase	Eutric Sodic Stagnic Regosol	< 1.0	Yes
P8	Mandarin	Setubalense	37.9675	-8.1808	529	5	Vase	Eutric Sodic Regosol	< 1.0	Yes
P9	Pomegranate	Acco	37.9644	-8.1841	666	5	Vase	Luvic Planosol	< 1.0	Yes

Note: * According to IUSS Working Group (2014).

Table 2
Main soil physical and chemical properties in the case studies.

Depth (m)	Soil texture (%)				OM (%)	ρ_b (Mg m^{-3})	Soil hydraulic properties (m^3 m^{-3})			TAW (mm)	EC_e (dS m^{-1})
	CS	FS	Si	C			θ_S	θ_{FC}	θ_{WP}		
P1. Almond											
0.0–0.3	46.0	23.7	15.4	14.9	2.2	1.33	0.419	0.225	0.067	99.5	0.21
0.3–0.5	35.2	16.6	13.2	35.0	0.8	1.41	0.388	0.215	0.135		0.29
0.5–1.0	27.6	13.1	13.1	46.2	0.4	-	-	-	-		0.34
P2. Almond											
0.0–0.2	41.0	28.0	17.1	13.9	2.0	1.48	0.418	0.195	0.080	120.6	0.20
0.2–0.4	27.8	20.0	13.4	38.8	1.1	1.41	0.421	0.202	0.080		0.18
0.4–0.7	12.5	20.5	12.0	55.0	0.8	-	-	-	-		0.19
0.7–1.0	35.5	31.8	15.9	16.8	-	-	-	-	-		0.47
P3. Olive											
0.0–0.4	19.9	38.7	21.1	20.3	1.2	1.34	0.458	0.198	0.105	74.0	0.20
0.4–0.6	21.9	33.9	21.5	22.7	1.0	-	-	-	-		0.14
0.6–0.8	23.8	31.9	19.2	25.1	0.6	-	-	-	-		0.23
P4. Olive											
0.0–0.4	27.1	38.5	17.7	16.7	2.6	1.36	0.409	0.192	0.075	116.7	0.20
0.4–0.7	27.3	19.1	10.2	43.4	0.7	-	-	-	-		0.10
0.7–1.0	32.0	10.6	7.5	49.9	1.7	-	-	-	-		0.26
P5. Olive											
0.0–0.5	15.7	16.4	20.0	48.0	1.5	1.38	0.543	0.469	0.295	139.1	0.24
0.5–0.8	29.6	20.0	22.5	27.9	0.3	-	-	-	-		0.22
P6. Orange											
0.0–0.7	39.4	34.5	13.1	13.0	0.9	1.50	0.409	0.252	0.100	136.8	0.51
0.7–0.9	28.2	23.8	14.9	33.1	3.8	-	-	-	-		0.33
P7. Clementine											
0.0–0.8	46.3	36.7	8.0	9.0	0.8	1.61	0.372	0.187	0.042	145.6	1.04
0.8–1.0	33.4	27.0	7.8	31.8	0.4	-	-	-	-		0.61
P8. Mandarin											
0.0–0.8	31.0	39.9	14.9	14.2	0.5	1.84	0.384	0.256	0.097	158.4	0.68
0.8–1.0	36.0	32.2	6.4	25.4	0.2	-	-	-	-		0.61
P9. Pomegranate											
0.0–0.6	49.6	37.6	7.2	5.6	1.5	1.51	0.382	0.195	0.045	149.7	0.38
0.6–0.8	44.1	31.2	7.3	17.4	1.4	-	-	-	-		0.17
0.8–1.0	42.5	37.1	6.9	13.5	0.5	-	-	-	-		0.13

Note: CS, coarse sand (2000–200 μm); FS, fine sand (200–20 μm); Si, silt (20–2 μm); C, clay (< 2 μm); ρ_b, soil bulk density; OM, soil organic matter; θ_S, θ_{FC}, θ_{WP}, soil water contents at saturation, field capacity, and the wilting point, respectively; TAW, total available water; EC_e, electrical conductivity of the saturation paste extract.

almond trees, the emitters, and the soil water monitoring points. Soil moisture data were subjected to calibration by comparing measured values with gravimetric soil water contents measured in disturbed soil samples taken periodically from each plot and multiplied by the respective ρ_b values. The soil water retention data determined in the laboratory was also considered in the calibration process. The continuous readings of soil water contents measured at different depths were then averaged for a daily value representing the entire soil profile. EC_e was periodically measured in each field by collecting disturbed soil samples below emitters using an auger. The monitored layer depths were 0.0–0.2, 0.2–0.4, 0.4–0.6, and 0.6–0.8 m, but reaching the deeper depths depended on the stoniness of soils of each plot and of soil moisture at sampling. Measured EC_e values were then averaged to get representative values of the rootzone salinity in the different fields. The electrical conductivity of irrigation water (EC_{iw}) was periodically monitored in the RID irrigation channel, with values averaging 0.72 dS m^{-1}. This value contrasts with the previous range of EC_{iw} values from 1.05 to 1.67 dS m^{-1} measured in the RDI channels between 2003 and 2006 (Martins et al., 2005), before the RDI was connected to Alqueva.

The crops were monitored for the crop stage dates, crop height (h), the fraction of the ground covered by the canopies (f_c), active root depth (Z_r), and interrow management. The dates of crop stages and respective growing degree-days (GDD) are given in Table 4. The dates of crop stages approach those reported in the literature for almond (Bellvert et al., 2018; López-López et al., 2018; Espadafor et al., 2015), olive (Garrido et al., 2021, 2020; Paço et al., 2019; Sanz-Cortés et al., 2002), citrus (Darouich et al., 2022b; García-Tejero et al., 2010, García Tejero et al., 2011; González-Altozano and Castel, 2000), and pomegranate (Intrigliolo et al., 2011; Melgarejo et al., 1997) grown in other locations also having a Mediterranean type of climate. The base temperatures

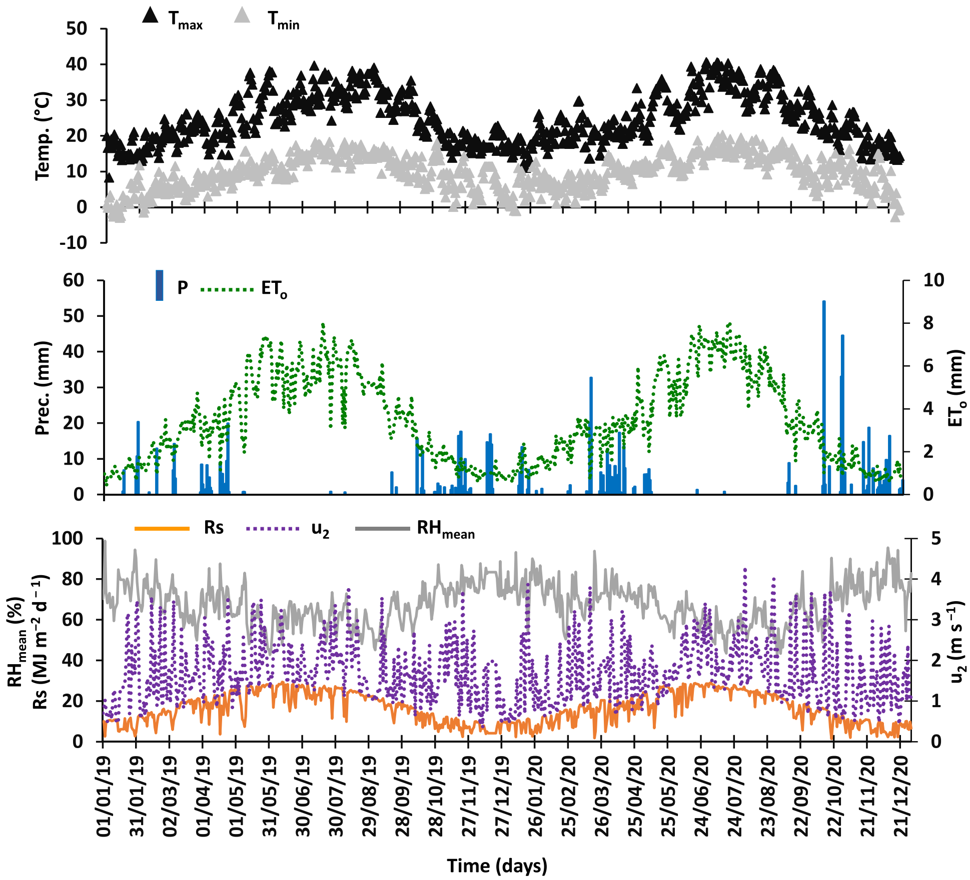

Fig. 2. Daily weather data during the study period (P, precipitation; ET_o, reference evapotranspiration; T_{max} and T_{min}, maximum and minimum air temperatures, respectively; RH_{mean}, mean relative humidity; Rs, solar radiation; u_2, wind speed at 2 m height).

Table 3
Seasonal irrigation and characteristics of irrigation events.

Plot	Dates		Depth per event (mm)			f_w (-)	Total (mm)
	Initiation	End	Mean	Minimum	Maximum		
P1. Almond							
2019	17/03	15/12	4.4	1.1	8.6	0.11	617
2020	05/03	26/11	3.9	1.0	10.5	0.11	596
P2. Almond							
2019	17/03	15/12	3.5	1.1	7.2	0.12	649
2020	05/03	26/11	5.0	1.7	13.0	0.12	772
P3. Olive							
2019	22/03	01/11	4.9	1.1	9.9	0.10	339
2020	29/01	18/10	6.1	1.2	9.2	0.10	355
P4. Olive							
2019	24/03	19/11	4.1	1.0	8.4	0.10	273
2020	28/03	17/10	3.5	1.0	6.3	0.10	266
P5. Olive							
2019	30/03	18/11	3.8	1.0	9.1	0.09	357
2020	10/03	18/10	4.0	1.0	8.5	0.09	330
P6. Orange							
2019	10/01	28/11	2.7	1.1	22.5	0.10	548
2020	10/03	15/10	5.9	1.9	12.2	0.18	843
P7. Clementine							
2019	18/01	09/12	3.3	1.1	20.1	0.12	653
2020	13/03	21/10	5.5	2.1	9.3	0.12	858
P8. Mandarin							
2019	18/01	09/12	4.7	1.0	9.3	0.10	906
2020	13/03	21/10	7.4	1.4	29.0	0.12	1170
P9. Pomegranate							
2019	11/03	03/12	4.7	1.1	8.5	0.17	654
2020	24/05	06/10	6.2	1.6	12.7	0.17	694

Note: f_w, fraction of the soil surface wetted by irrigation.

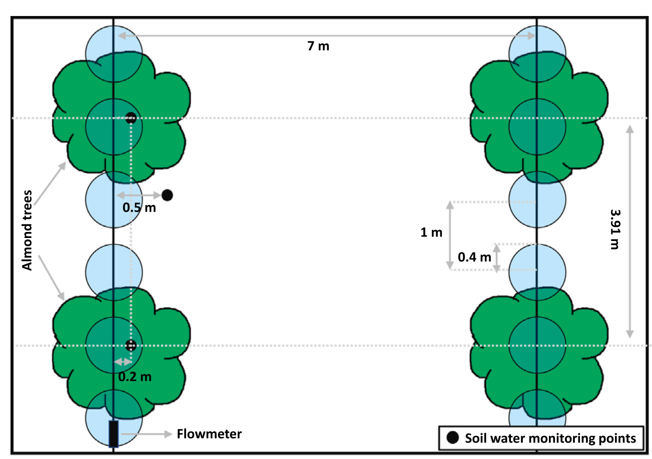

Fig. 3. Experimental layout in the P1 plot.

considered for computing the GDD were 7.0 ºC for almond (Egea et al., 2003; Degrandi-Hoffman et al., 1996), 8.8 ºC for olive (Melo-Abreu et al., 2004), 12.8 °C for citrus (Darouich et al., 2022b; Luo, 2011; Coops et al., 2001), and 10ºC for pomegranate (Melgarejo et al., 1997), again in line with the respective literature.

Tree height (Table 5) and mean canopy width were monitored using a tape at the beginning of the initial, mid-season, and late-season, as well as the non-growing season. The f_c values are presented in Table 5 and refer to the average values observed in each crop stage since no significant differences were found between the two monitored seasons. Trees in plots P1 and P2 (almond fields) were subjected to a light pruning at

Table 4
Crop growth stage dates and duration of growing seasons (in growing degree-days, GDD).

Plot		Crop growth stages							Total GDD (ºC)
		Non-growing	Initiation	Crop develop.	Mid-season	Late-season	End-season	Non-growing	
P1. Almond									
2019	Dates	01/01	22/02	04/03	24/03	30/08	01/11	31/12	-
	GDD	-	66	126	2107	866	-	-	3165
2020	Dates	01/01	18/02	01/03	20/03	27/08	05/11	31/12	-
	GDD	-	72	131	2202	894	-	-	3299
P2. Almond									
2019	Dates	01/01	22/02	04/03	24/03	30/08	01/11	31/12	-
	GDD	-	66	126	2107	866	-	-	3165
2020	Dates	01/01	18/02	01/03	20/03	27/08	05/11	31/12	-
	GDD	-	72	131	2202	894	-	-	3299
P3. Olive									
2019	Dates	01/01	05/03	20/03	14/05	25/09	01/11	31/12	-
	GDD	-	67	378	1833	379	-	-	2657
2020	Dates	01/01	01/03	20/03	18/05	25/09	01/11	31/12	-
	GDD	-	96	397	1935	322	-	-	2750
P4. Olive									
2019	Dates	01/01	08/03	19/03	10/05	30/09	15/11	31/12	-
	GDD	-	52	331	1942	392	-	-	2717
2020	Dates	01/01	05/03	20/03	12/05	25/09	12/11	31/12	-
	GDD	-	79	348	1983	396	-	-	2806
P5. Olive									
2019	Dates	01/01	05/03	19/03	10/05	25/09	05/11	31/12	-
	GDD	-	63	331	1884	413	-	-	2691
2020	Dates	01/01	05/03	24/03	14/05	01/10	20/11	31/12	-
	GDD	-	88	352	2034	401	-	-	2875
P6. Orange									
2019	Dates	01/01	22/02	20/03	20/05	25/10	31/12	-	-
	GDD	-	25	204	1435	114	-	-	1778
2020	Dates	01/01	24/02	25/03	23/05	15/11	31/12	-	-
	GDD	-	36	218	1580	60	-	-	1894
P7. Clementine									
2019	Dates	01/01	22/02	17/03	15/05	28/10	31/12	-	-
	GDD	-	24	180	1482	92	-	-	1778
2020	Dates	01/01	24/02	20/03	23/05	04/11	31/12	-	-
	GDD	-	35	219	1550	89	-	-	1893
P8. Mandarin									
2019	Dates	01/01	22/02	15/03	15/05	23/10	31/12	-	-
	GDD	-	21	183	1458	116	-	-	1778
2020	Dates	01/01	24/02	20/03	23/05	04/11	31/12	-	-
	GDD	-	35	219	1550	89	-	-	1893
P9. Pomegranate									
2019	Dates	01/01	22/03	12/04	10/05	15/10	25/11	31/12	-
	GDD	-	83	177	1924	207	-	-	2391
2020	Dates	01/01	27/03	16/04	15/05	07/10	15/11	31/12	-
	GDD	-	96	186	1901	266	-	-	2449

Table 5
Mean values of the fraction of the ground cover (f_c), tree height (h), and root depth (Z_r) during the diverse crop stages.

Plot	Crop stages								Z_r (m)
	Non-growing		Initiation		Mid-season		End-season		
	f_c (-)	h (m)	f_c (-)	h (m)	f_c (-)	h (m)	f_c (-)	h (m)	
P1. Almond	0.08	3.0	0.10	3.0	0.41	4.0	0.20	4.0	1.0
P2. Almond	0.05	3.0	0.10	3.0	0.42	4.0	0.20	4.0	1.0
P3. Olive	0.24	4.0	0.24	4.0	0.26	4.1	0.23	4.0	0.8
P4. Olive	0.20	2.8	0.20	2.8	0.23	3.0	0.20	2.8	1.0
P5. Olive	0.20	3.8	0.22	3.8	0.27	3.9	0.23	3.8	0.8
P6. Orange	0.29	2.4	0.29	2.4	0.29	2.4	0.29	2.4	1.0
P7. Clementine	0.25	2.7	0.25	2.7	0.28	2.7	0.28	2.7	1.0
P8. Mandarin	0.28	2.8	0.28	2.8	0.29	2.8	0.28	2.8	1.0
P9. Pomegranate	0.05	2.0	0.20	2.0	0.41	2.5	0.30	2.3	1.0

the beginning of January 2020. Trees in plots P3 and P4 (olive fields) were pruned more intensively in February 2020. Z_r was assessed from observations in soil profiles. Lastly, the interrow were monitored for the periods with active groundcover, and for residues mulching when those plants dried out by the early summer. The density and height of the interrow plants was assessed by visual analysis, and the fraction of the ground covered by those plants ($f_{c\ cover}$) was defined accordingly.

2.3. Modeling approach

2.3.1. Model description

The soil water balance SIMDualKc model (Rosa et al., 2012) has been extensively described in several publications, namely relative to its use (e.g., Pereira et al., 2015a, 2020b; Paço et al., 2019; Darouich et al., 2022a, 2022b). Therefore, only the main features of the modeling approach are given here. The soil water balance at the field scale is performed daily as follows:

$$D_{r,i} = D_{r,i-1} - (P - RO)_i - I_i - CR_i + DP_i + ET_{c\ act,i} \quad (1)$$

where D_r is the root zone depletion (mm) given by the difference between soil water content at field capacity and actual soil moisture conditions, P is the rainfall (mm), RO is the runoff (mm), I is the net irrigation depth (mm), CR is the capillary rise from the groundwater table (mm), DP is the deep percolation (mm), and $ET_{c\ act}$ is the actual crop evapotranspiration (mm), all referring to day i or i-1. In this application, CR was not considered as the groundwater table was too deep (>4.2 m) to contribute to crop evapotranspiration.

Following the FAO56 dual-K_c approach (Allen et al., 1998, 2005; Pereira et al., 2020b), the ET_c (mm) is estimated by computing the components relative to crop transpiration (T_c, mm) and soil evaporation (E_s, mm) separately:

$$T_c = K_s K_{cb} ET_o \quad (2)$$

$$E_s = K_e ET_o \quad (3)$$

where K_{cb} is the standard basal crop coefficient (-) that refers primarily to crop transpiration although some diffusive soil evaporation may also be included, particularly during the initial crop stage, K_e is the evaporation coefficient (-) that describes direct evaporation from the surface soil layer of depth Z_e (cm), ET_o is the reference evapotranspiration (mm) computed with the FAO Penman-Monteith equation (Allen et al., 1998), and K_s is a multiplier stress coefficient describing the impact of water and salinity stressors on crop evapotranspiration. $K_s = 1$ when no stress occurs and actual crop transpiration rates ($T_{c\ act}$, mm) match their potential values (T_c, mm); $K_s < 1$, and $T_{c\ act} < T_c$, when crops are subjected to water and/or salinity stress. In this application, the K_s was computed following Pereira et al. (2007) and Minhas et al. (2020):

$$K_s = \left(\frac{TAW_{salt} - D_r}{TAW_{salt} - RAW_{salt}}\right)\left(1 - \frac{b}{K_y 100}(EC_e - EC_{e\ threshold})\right) \quad (4)$$

where TAW_{salt} and RAW_{salt} are the total and readily available water (mm) corrected for salinity relative to the root zone soil depth Z_r (m), $EC_{e\ threshold}$ is the crop tolerance salinity threshold value (dS m^{-1}) where crop growth and production starts to decline, b is the percentage of crop yield reduction per unit increase in EC_e above the $EC_{e\ threshold}$ (%/dS m^{-1}), and K_y is the yield response factor (-) that describes the relationship between the relative yield decrease and the relative evapotranspiration deficit (Stewart et al., 1977; Doorenbos and Kassam, 1979). Parameter values were updated by Minhas et al. (2020). The first term on the right side of the previous equation corresponds to the water (matric) stress when $D_{r,i} > RAW_{salt}$. The second one is used to correct the former for the effects of salinity (osmotic) stress, i.e., when $EC_e > EC_{e\ threshold}$ relative to the considered crop as follows:

$$TAW_{salt} = (\theta_{FC} - \theta_{WP\ salt})1000\, Z_r \quad (5)$$

$$RAW_{salt} = p_{salt} TAW \quad (6)$$

and

$$\theta_{WP\ salt} = \theta_{WP} + \frac{b}{100}\left(\frac{EC_e - EC_{e\ threshold}}{10}\right)(\theta_{FC} - \theta_{WP}) \quad (7)$$

$$p_{salt} = p - b(EC_e - EC_{e\ threshold})p \quad (8)$$

where θ_{FC} is the soil water content at the field capacity ($m^3\ m^{-3}$), θ_{WP} is the soil water content at the wilting point ($m^3\ m^{-3}$), Z_r is the crop root depth (m), and $\theta_{WP\ salt}$ and p_{salt} are respectively the soil water content at the wilting point and the depletion fraction for no stress (p) after correction for salinity. Successful applications of this approach can be found in Rosa et al. (2016) for maize and sorghum in Portugal, and Liu et al. (2022a, 2022b) for maize in China.

Soil evaporation is computed through consideration of the energy available at the soil surface and water availability in the evaporative soil layer. The two-stage evaporation model of Ritchie (1972) is adopted, with the first stage corresponding to the energy limited stage, and the second to the water limited stage (Allen et al., 1998, 2005; Pereira et al., 2020b). In this approach, the K_e is computed as:

$$K_e = K_r(K_{c\ max} - K_{cb\ min}) \le f_{ew} K_{c\ max} \quad (9)$$

and K_r as follows:

$$K_r = 1 \quad \text{for} \quad D_{e,i-1} \le REW \quad (10)$$

$$K_r = \frac{TEW - D_{e,i-1}}{TEW - REW} \quad \text{for} \quad D_{e,i-1} > REW \quad (11)$$

where K_r is the evaporation reduction coefficient (-), $K_{c\ max}$ is the maximum value of K_c (i.e., $K_{cb} + K_e$) following rain or irrigation events (−), f_{ew} is the fraction of the soil that is both exposed to solar radiation and wetted by rain or irrigation, and which depends upon the effective fraction of ground covered or shaded by vegetation near solar noon ($f_{c\ eff}$), TEW is the maximum depth of water that can be evaporated from the evaporation soil layer when it has been completely wetted (mm), REW is the depth of water that can be easily evaporated without water availability restrictions (mm), and D_e is the evaporation layer depletion at the end of day $i - 1$ (mm). The computation of D_e implies computing the daily soil water balance for the evaporative soil layer.

Deep percolation (DP) is estimated using a time decay function relating the soil water storage near saturation with the time after the occurrence of heavy rain or irrigation (Liu et al., 2006):

$$W_a = a_D\, t^{b_D} \quad (12)$$

where W_a is the actual soil water storage in the root zone (mm), a_D is the soil water storage comprised between θ_S and θ_{FC}, b_D is an empirical dimensionless parameter (-), and t is the time after irrigation or rain that produces storage above field capacity (days). Surface runoff is estimated using the widely used curve number (CN) approach (Allen et al., 2007; USDA-SCS, 1972).

For tree crops and vineyards, the K_{cb} values include the characteristics of the main crop and the understory vegetation. While they are obtained from model calibration, the K_{cb} values can be divided into their components as follows (Pereira et al., 2020a, 2021c; Allen and Pereira, 2009):

$$K_{cb} = K_{cb\ gcover} + K_d\left(\max\left(K_{cb\ full} - K_{cb\ gcover}, \frac{K_{cb\ full} - K_{cb\ gcover}}{2}\right)\right) \quad (13)$$

where $K_{cb\ gcover}$ is the K_{cb} of the ground cover vegetation in the absence of tree foliage (-), $K_{cb\ full}$ is the estimated basal K_c during peak plant growth for conditions having nearly full ground cover (-), and K_d is the crop density coefficient (-). The second term of the max function reduces the estimate for K_{cb} during the mid-season stage by half the difference between $K_{cb\ full}$ and $K_{cb\ cover}$ when this difference is negative. This accounts for impacts of the shading of the surface cover by overstory vegetation having a K_{cb} that is lower than that of the ground cover due to differences in stomatal conductance. When no ground cover exists or when the cover crop dries out becoming a less dense residual mulch, the previous equation is simplified by replacing $K_{cb\ cover}$ with the minimum K_c for bare soil ($K_{c\ min} = 0.15$). The $K_{cb\ full}$ is estimated primarily as a function of crop height and then adjusted for tree crops using a reduction factor (F_r) estimated from the mean leaf stomatal resistance (Pereira et al., 2020a). The density coefficient (K_d) is estimated from the fraction of ground cover as follows:

$$K_d = \min\left(1, M_L f_{c\ eff}, f_{c\ eff}^{\left(\frac{1}{1+h}\right)}\right) \quad (14)$$

where $f_{c\ eff}$ is the effective fraction of ground covered or shaded by vegetation near solar noon (-), M_L is a multiplier on $f_{c\ eff}$ (1.5–2.0) describing the effect of the canopy density on shading and on maximum relative evapotranspiration per fraction of ground shaded (to simulate the physical limits imposed on water flux through the plant root, stem, and leaf systems), and h is the mean height of trees (m). Successful applications of this approach can be found in Darouich et al. (2022a), (2022b) for grapevine and citrus, and Paço et al., (2019, 2014) for olive.

2.3.2. Model setup

The computation of the soil water balance in each study orchard required comprehensive data on weather conditions, soil properties, crop phenology, ground conditions (active ground cover and/or mulch), irrigation events, and performance of irrigation systems to feed the SIMDualKc model.

Soil data included the particle size distribution and θ_{FC} and θ_{WP} of the different layers in each soil profile, as well as the mean EC_e of the entire rootzone (Table 2). TAW_{salt} was then computed as the sum of the product of the difference between θ_{FC} and θ_{WP} relative to the different soil layers of the rootzone of depth Z_r (Table 5) while adjusting to salinity conditions when $EC_e > EC_{e\ threshold}$ (Minhas et al., 2020; Rosa et al., 2016). This adjustment was specified for the initial conditions and the dates when EC_e data was available from sampling. Then, TAW_{salt} (and the corresponding RAW_{salt}) varied linearly between two successive dates depending on whether salinity levels were above crop tolerance thresholds along the growing seasons. If these conditions were not observed, no salinity adjustment was required. The TEW, REW, and the depth of the evaporative soil layer (Z_e, m) were set up according to the textural and hydraulic properties of the surface soil layer (Allen et al., 1998, 2005). The deep percolation parameters a_D and b_D were defined according to soil texture and soil hydraulic properties (Liu et al., 2006). The CN values for computing runoff were set up based on the texture of the surface soil layer, soil surface conditions, and land use (USDA-SCS, 1972). Lastly, the initial soil water depletion values in both the root zone and the evaporative soil layer corresponded to field measurements (Table 6).

Crop data included the observed dates of the initial, development, mid-season, and late-season stages, as well as the non-growing periods (Table 4). Also included were the corresponding K_{cb} values for the initial ($K_{cb\ ini}$), mid-season ($K_{cb\ mid}$), end season ($K_{cb\ end}$), and non-growing periods ($K_{cb\ non\ growing}$). The K_{cb} default values were computed following Pereira et al. (2021c) by considering the management system in each orchard, and the f_c and h measured in each crop stage (Table 5). For each management class, the central F_r value of the proposed range of values was selected. The soil water depletion fraction values for no stress for the same crop stages (p_{ini}, p_{mid}, p_{end}) were set up following Allen et al. (1998). Crop state variables such as h, f_c, and Z_r were defined for each crop stage according to observations (Table 5). Lastly, the K_y, $EC_{e\ threshold}$, and b values were taken from the literature (Ayers and Westcot, 1985; Allen et al., 1998; Minhas et al., 2020). For almonds, the K_y was 0.70, the $EC_{e\ threshold}$ was 1.5 dS m^{-1}, and b was 19%/dS m^{-1}. For olive and pomegranate, the K_y was 0.75, the $EC_{e\ threshold}$ was 4.0 dS m^{-1}, and b was 16%/dS m^{-1}. For citrus, K_y was 1.20, the $EC_{e\ threshold}$ was 1.7 dS m^{-1}, and b was 16%/dS m^{-1}.

Ground cover conditions were defined based on observations and included the periods with active ground cover, usually during the rainy season (i.e., from October to May) and with residues mulching due to falling leaves or when the row and interrow weeds dried out. In almond plots (P1 and P2), the active ground cover was present only in the interrow, with a density of 20%, a fraction of ground cover ($f_{c\ cover}$) of 0.30, and a maximum height (h_{cover}) of 0.15 m. In olive plots (P3 and P4), the density of the active ground cover in the interrow ranged from 20% to 30%, and the $f_{c\ cover}$ varied from 0.20 to 0.30, with h_{cover} of 0.25. Lower values were always observed in P3. In both fields, there was only a residual presence of active ground cover along the trees row. No active ground cover was observed in the P5 olive plot. In citrus (P6, P7, and P8) and pomegranate (P9) plots, the density of the active ground cover in the row and interrow varied from 20% to 50%, the $f_{c\ cover}$ was from 0.20 to 0.50, and the h_{cover} was from 0.20 m (P7) to 0.50 m (P9). In all fields, the evaporation reduction due to the residues mulch was ranging from 40% (P1 and P2) to 60% (P9).

The dates of irrigation events and depths applied were input according to observations. The fractions of the soil surface wetted by irrigation (f_w) were also defined according to field measurements (Table 3).

Table 6
Initial soil water depletion in the root zone (% of TAW) and evaporable soil layer (% of TEW).

Plot	% of TAW	% of TEW
P1. Almond		
2019	9.0	9.0
2020	0.0	0.0
P2. Almond		
2019	0.0	0.0
2020	0.0	0.0
P3. Olive		
2019	41.0	41.0
2020	20.0	20.0
P4. Olive		
2019	45.0	45.0
2020	31.0	31.0
P5. Olive		
2019	45.0	45.0
2020	30.0	30.0
P6. Orange		
2019	8.0	8.0
2020	5.0	5.0
P7. Clementine		
2019	6.0	6.0
2020	5.0	5.0
P8. Mandarin		
2019	13.0	13.0
2020	7.0	7.0
P9. Pomegranate		
2019	10.0	10.0
2020	7.0	7.0

2.3.3. Model calibration and validation

The SIMDualKc model followed the same "iterative trial-and-error" procedure described in Pereira et al. (2015b), which consists of adjusting groups of combined model parameters, one at a time and within reasonable ranges of values until deviations between model simulations and field measurements of soil water contents in the rootzone are minimized. Calibration was carried out for each of the studied orchards using the 2019 dataset. Validation was then performed using the calibrated parameters and the 2020 dataset. Model calibration started by first adjusting the K_{cb} and the corresponding p-values for each crop stage; then, the a_D and b_D parameters of Liu et al. (2006) parametric functions, followed by Z_e, TEW, and REW; and lastly, the CN value. The $EC_{e\ threshold}$, b, and K_y model parameters did not require adjustment. Model calibration ended when the best fit was reached, i.e., when the errors of prediction did not change from one iteration to the next. If that goal was not achieved at the end of a modification cycle, the calibration process restarted again.

The statistical indicators used to evaluate the goodness-of-fit between observed (O_i) and predicted (P_i) soil water content values were also those proposed and described by Pereira et al. (2015b): the regression coefficient of the linear regression through the origin (b_0), the coefficient of determination (R^2) of the ordinary least-squares regression between observed and predicted values, the root mean square error (RMSE), the ratio of the RMSE to the standard deviation of the observed data (NRMSE), the percent bias of estimation (PBIAS), and the modeling efficiency (NSE). The full description of these indicators can be found in Moriasi et al. (2007), Legates and McCabe (1999), and Nash and Sutcliffe (1970). In general, b_0 equal to 1 indicates that the predicted values are statistically identical to field measurements. R^2 values close to 1 show that the model well explains the variance of the observations. RMSE and NRMSE values close to zero indicate that estimation errors are small and model predictions are excellent. PBIAS values close to zero describe accurate model simulations, while negative or positive values indicate over- or under-estimation bias, respectively. NSE values close to 1 mean that model predictions are good because the residuals' variance is much smaller than the observed data variance. Contrarily, if NSE < 0, the observed mean is a better estimator than model predictions.

3. Results and discussion

3.1. Model parametrization

Table 7 presents the calibrated model parameters relative to the nine case studies. The default K_{cb} values for the initial, mid-, and end-of-season stages were set up following Pereira et al. (2021c), by considering the characteristics that most approached crop management in each field as well as the f_c and h values measured in each crop stage. However, as the K_{cb} values are much dependent on observed values of f_c and h (Pereira et al., 2020a, 2021c), as well as on interrow management (Darouich et al., 2022a), the calibrated ones ended up varying to a greater or lesser extent from the default values.

In olive trees, the calibrated fractions of soil water depletion for no-stress (p values) were always below those proposed by Allen et al. (1998) for the different crop stages. They were also lower than those in Paço et al. (2019) but higher than in Santos (2018). In almonds, only the p_{ini} and p_{mid} values differed from Allen et al. (1998), larger in both cases. On the other hand, the calibrated p values in citrus and pomegranate orchards always matched those in Allen et al. (1998). The remaining calibrated parameters, i.e., the soil evaporation parameters Z_e, TEW, and REW; the percolation parameters a_D and b_D from Liu's et al. (2006) parametric equations; and the CN value for computing runoff, were found to have values in agreement with the soil textural and the soil hydraulic characteristics of each case study field.

3.2. Model performance

Fig. 4 and Fig. 5 show the fitting of the daily measured soil water contents (SWC) by the SIMDualKc-simulated values in the nine commercial orchards during the 2019 and 2020 growing seasons. The figures also include the depths and dates of irrigation and rainfall events. The figures further reflect the diverse management applied in the monitored fields.

In the almond fields (Fig. 4), the SWC dynamics differed between sites, with SWC in P1 dropping below θ_p in both seasons. Soil salinity

Table 7
Initial default (in brackets) and calibrated model parameters.

Parameter	P1 Almond	P2 Almond	P3 Olive	P4 Olive	P5 Olive	P6 Orange	P7 Clementine	P8 Mandarin	P9 Pomegranate
$K_{cb\ non\ growing}$	0.18 (0.20)	0.18 (0.20)	0.32 (0.32)	0.32 (0.32)	0.33 (0.32)	0.41 (0.40)	0.40 (0.40)	0.40 (0.40)	0.26 (0.20)
$K_{cb\ ini}$	0.22 (0.20)	0.22 (0.20)	0.32 (0.32)	0.32 (0.32)	0.33 (0.32)	0.40 (0.40)	0.40 (0.40)	0.40 (0.40)	0.24 (0.34)
$K_{cb\ mid}$	0.58 (0.60)	0.58 (0.60)	0.35 (0.38)	0.35 (0.38)	0.36 (0.38)	0.41 (0.41)	0.40 (0.41)	0.40 (0.41)	0.60 (0.64)
$K_{cb\ end}$	0.50 (0.40)	0.50 (0.40)	0.33 (0.31)	0.33 (0.31)	0.34 (0.31)	0.41 (0.41)	0.40 (0.41)	0.40 (0.41)	0.52 (0.41)
p_{ini}	0.60 (0.40)	0.60 (0.40)	0.55 (0.65)	0.50 (0.65)	0.50 (0.65)	0.50 (0.50)	0.50 (0.50)	0.50 (0.50)	0.50 (0.50)
p_{mid}	0.45 (0.40)	0.45 (0.40)	0.55 (0.65)	0.50 (0.65)	0.50 (0.65)	0.50 (0.50)	0.50 (0.50)	0.50 (0.50)	0.50 (0.50)
p_{end}	0.60 (0.60)	0.60 (0.60)	0.55 (0.65)	0.50 (0.65)	0.50 (0.65)	0.50 (0.50)	0.50 (0.50)	0.50 (0.50)	0.50 (0.50)
TEW (mm)	19 (24)	19 (23)	16 (22)	19 (16)	26 (32)	20 (29)	13 (25)	15 (31)	17 (26)
REW (mm)	9 (9)	10 (10)	8 (9)	10 (9)	9 (12)	9 (9)	6 (7)	8 (9)	7 (7)
Z_e (m)	0.10 (0.10)	0.12 (0.15)	0.10 (0.15)	0.11 (0.10)	0.10 (0.15)	0.10 (0.15)	0.10 (0.15)	0.10 (0.15)	0.10 (0.15)
a_D (mm)	225 (-)	220 (-)	210 (-)	200 (-)	420 (-)	265 (-)	200 (-)	267 (-)	215 (-)
b_D	– 0.019 (−0.0173)	– 0.018 (−0.0173)	– 0.020 (−0.0173)	– 0.020 (−0.0173)	– 0.018 (−0.0173)	– 0.020 (−0.0173)	– 0.020 (−0.0173)	– 0.020 (−0.0173)	– 0.018 (−0.0173)
CN	68 (72)	68 (72)	75 (72)	80 (72)	75 (80)	70 (72)	75 (72)	70 (72)	70 (65)

Symbols: K_{cb}, basal crop coefficients for the initial ($K_{cb\ ini}$), mid ($K_{cb\ mid}$), and end season ($K_{cb\ end}$); $K_{cb\ non\ growing}$, basal crop coefficient during the non-growing period; p, depletion fraction for no stress during the initial (p_{ini}), mid (p_{mid}), and end season (p_{end}); TEW, total evaporable water; REW, readily evaporable water; Z_e, depth of the soil evaporation layer; a_D and b_D, parameters of the deep percolation; CN, curve number.

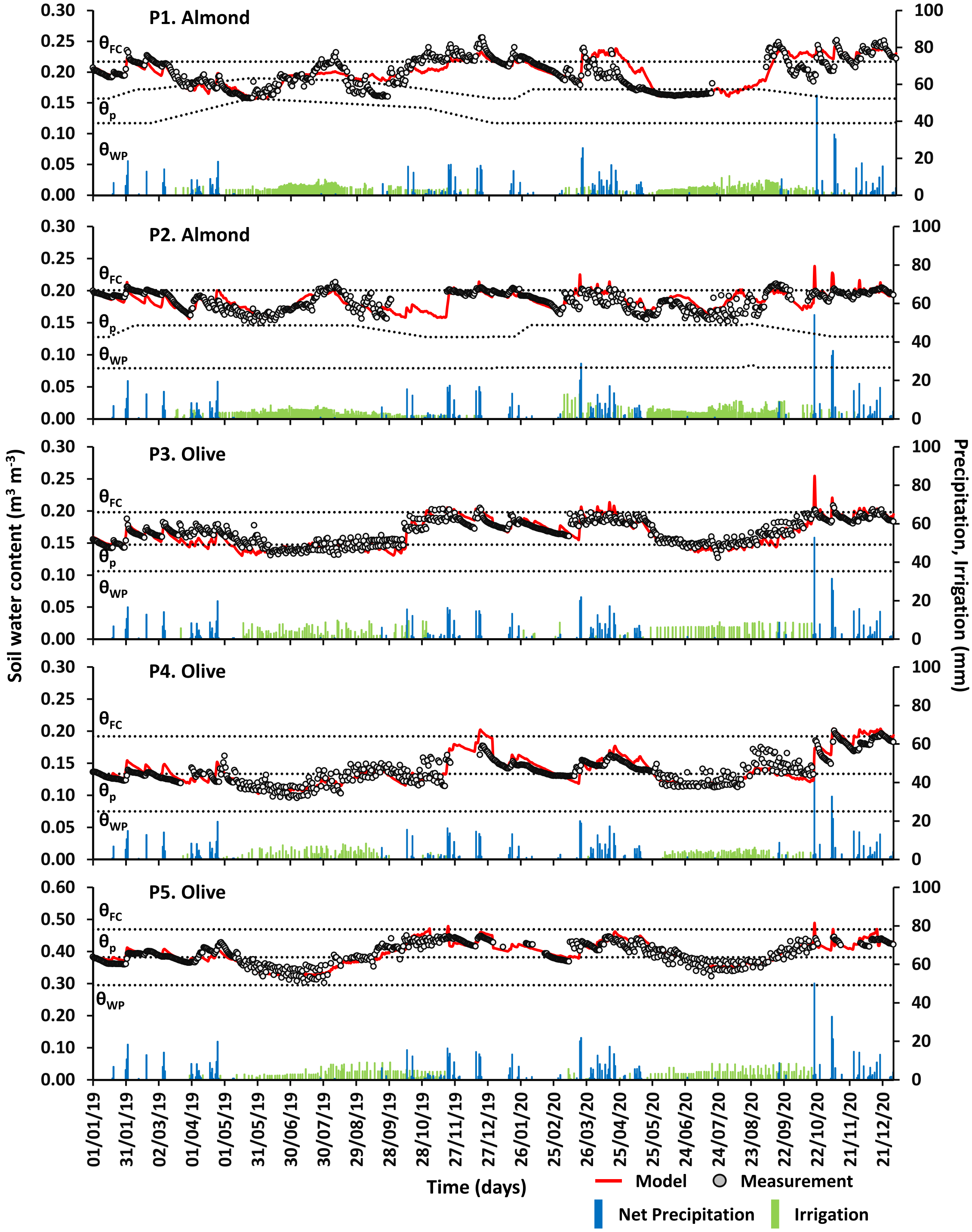

Fig. 4. Measured and simulated soil water contents in plots P1, P2, P3, P4, and P5 during the 2019–2020 growing seasons (θ_{FC}, θ_{WP}, and θ_p correspond to soil water contents at field capacity, the wilting point, and at the depletion fraction for no stress).

was monitored in 2019, a dry year, which partially explains that SWC drop below θ_p. In P2, the measured EC_e values were never above the $EC_{e\ threshold}$ for almonds and the SWC values were always kept within the RAW limits. In the olive fields (Fig. 4), the SWC also dropped to values below θ_p for extended periods during both irrigation seasons, which indicates that trees were subjected to mild water stress during most of the mid- and late-season stages. No salinity stress was ever noticed in these sites. Contrastingly, SWC in citrus fields (Fig. 5) were systematically above θ_{FC} during irrigation periods, thus clearly showing that over-irrigation was practiced. This assumption was confirmed when observing Table 3, which shows that high water depths were applied over both seasons, especially in the mandarin field (P8). The same was observed in the pomegranate case in 2020, where SWC was continuously monitored above θ_{FC} during the irrigation season. The results above indicate that farmers adopt a poor irrigation scheduling and that there is the need to develop and propose to farmers the adoption of water saving schedules as the ones presented later.

The box plots in Fig. 6 present the mean EC_e values measured in all fields along the two seasons. Results differ from a plot to another, and their variability is supposed to differently influence soil water

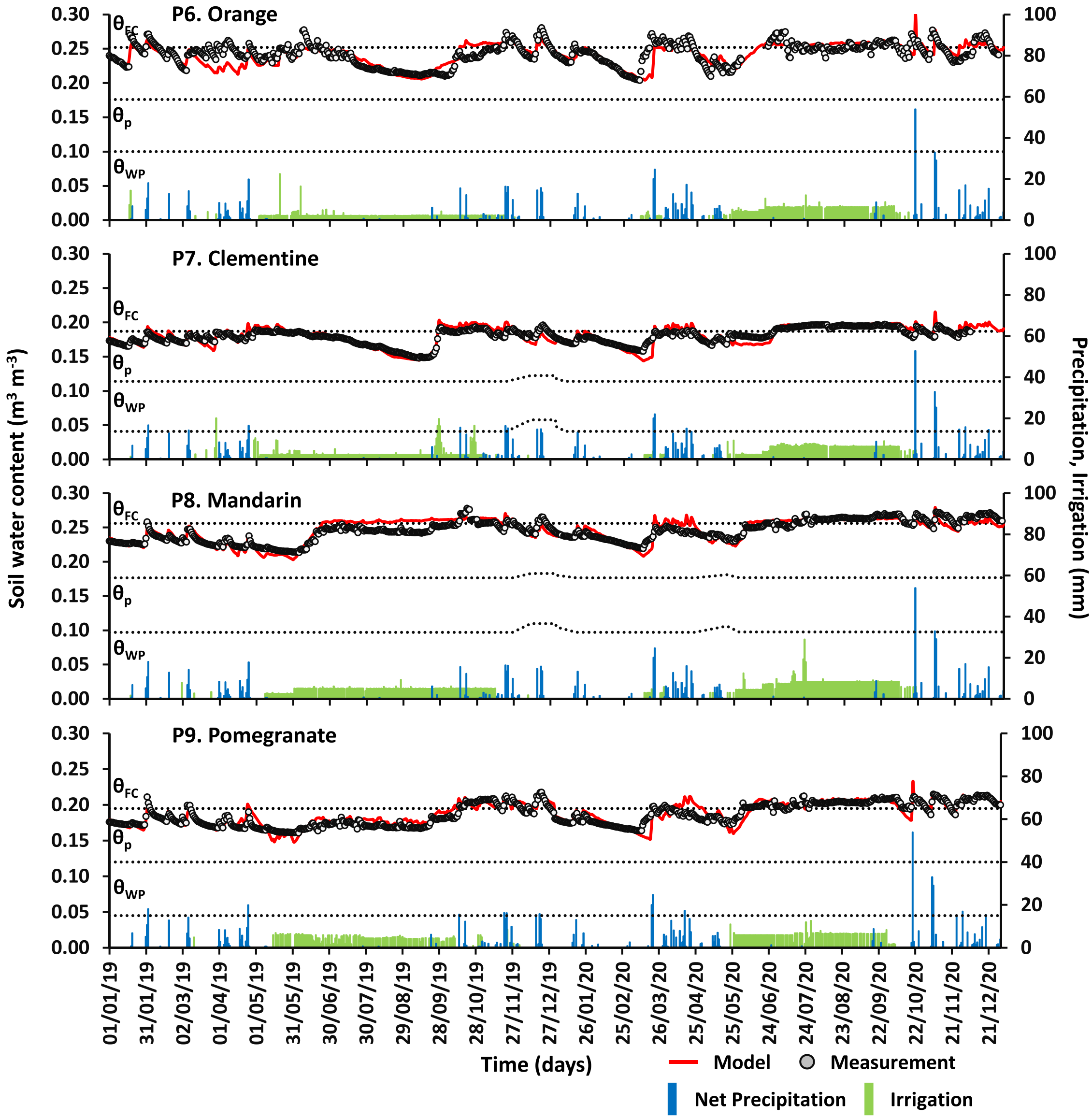

Fig. 5. Measured and simulated soil water contents in plots P6, P7, P8, and P9 during the 2019–2020 growing seasons (θ_{FC}, θ_{WP}, and θ_p correspond to soil water contents at field capacity, the wilting point, and at the depletion fraction for no stress).

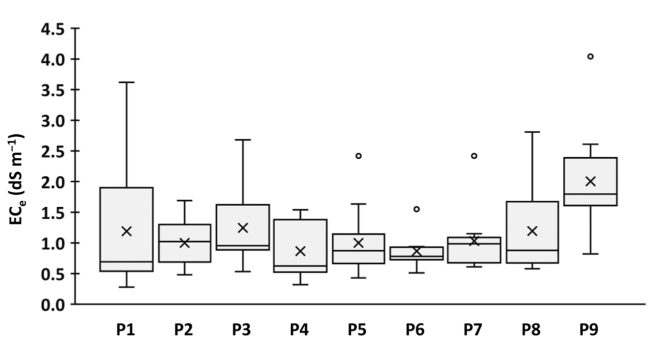

Fig. 6. Box-plots of mean values of the electrical conductivity of the soil saturation paste extract (EC_e) measured in the rootzone of almond (P1 and P2), olive (P3, P4, and P5), citrus (P6, P7, and P8), and pomegranate (P9) orchards during the 2019 and 2020 growing seasons (X represents the mean while the bar ▬▬ represents the median value).

availability. P1 was greatly affected by soil salinity, mainly during the 2019 season, so affecting the almond crop, which is sensitive to soil salinity ($EC_{e\ threshold}$ = 1.5 dS m^{-1}). In this field, EC_e measurements performed along the season were systematically higher than the crop tolerance salinity threshold (3.62 dS m^{-1} on May 24th, 2019; 2.80 dS m^{-1} on October 31st, 2019; and 1.90 dS m^{-1} on December 12th, 2019), resulting in an increase of the osmotic stress and decrease of soil water availability. In all other fields, soil salinity did not increase to levels above the crop tolerance thresholds except for some short periods in case of P2 (1.69 dS m^{-1} on August 24th, 2020), P7 (2.42 dS m^{-1} on December 11th, 2019), and P8 (2.81 dS m^{-1} on December 11th, 2019; and 2.06 dS m^{-1} on May 5th, 2020). P9, in a Luvic Planosol, i.e., where the soil has the poorest drainage conditions among all case studies, registered the highest salinity levels (4.04 dS m^{-1} on December 11th, 2019) but, because pomegranate is highly tolerant to salinity stress, there was no noticeable impact on SWC.

The statistical indicators used to evaluate the goodness-of-fit between simulated and measured SWC values are presented in Table 8. For the calibration year (2019), the regression coefficients b_0 were all close to the 1.0 target, ranging from 0.98 (P1) to 1.02 (P8), indicating that the

Table 8
Goodness-of-fit indicators when comparing measured and simulated soil water contents. Data for the calibration were those of 2019 and for validation those of 2020.

Plot	b_0 (-)	R^2 (-)	RMSE (m^3 m^{-3})	NRMSE (-)	PBIAS (%)	NSE (-)
P1. Almond						
2019	0.978	0.729	0.003	0.016	1.718	0.694
2020	1.027	0.671	0.005	0.024	-3.079	0.586
P2. Almond						
2019	0.991	0.593	0.002	0.009	0.692	0.584
2020	1.018	0.449	0.002	0.013	-2.150	0.363
P3. Olive						
2019	0.980	0.768	0.002	0.019	2.041	0.644
2020	0.997	0.822	0.001	0.015	0.440	0.723
P4. Olive						
2019	1.003	0.577	0.002	0.019	-0.486	0.408
2020	1.005	0.799	0.003	0.018	-0.385	0.699
P5. Olive						
2019	0.991	0.820	0.005	0.013	0.887	0.782
2020	1.008	0.768	0.004	0.010	-0.836	0.720
P6. Orange						
2019	0.991	0.534	0.003	0.011	0.799	0.468
2020	1.003	0.513	0.003	0.010	-0.406	0.458
P7. Clementine						
2019	1.008	0.842	0.001	0.004	-0.731	0.671
2020	1.005	0.784	0.001	0.005	-0.441	0.521
P8. Mandarin						
2019	1.015	0.815	0.002	0.006	-1.432	0.587
2020	0.998	0.744	0.001	0.004	0.177	0.718
P9. Pomegranate						
2019	1.013	0.779	0.001	0.006	-1.395	0.724
2020	1.004	0.707	0.001	0.007	-0.423	0.619

Note: b_0, regression coefficient; R^2, coefficient of determination; RMSE, root mean square error; NRMSE, ratio of the RMSE to the standard deviation of observed data; PBIAS, percent bias; NSE, model efficiency.

simulated values were close to the observed ones. The value of R^2 varied from 0.53 (P6) to 0.84 (P7), showing that generally the model could explain most of the variance of the observed data. The errors of the estimates were always small ($0.001 \leq \text{RMSE} \leq 0.005$ m^3 m^{-3} and $0.004 \leq \text{NRMSE} \leq 0.019$). In agreement with b_0, the PBIAS values were quite small ($-1.43 \leq \text{PBIAS} \leq 2.04\%$), with no particular over- or under-estimation trend in simulating the measured data. Lastly, the NSE values were relatively high, ranging from 0.408 (P4) to 0.782 (P5), thus indicating that the variance of the residuals was smaller than the measured data variance. For validation (with 2020 data), the goodness-of-fit indicators showed generally the same trend and similar range of values as observed for calibration. The worst statistics were obtained in P2 while the best indicators were in P3.

Hence, overall, the SIMDualKc model performed well when simulating SWC in the nine case studies relative to the four tree crops. The resulting goodness-of-fit indicators were also within the ranges of values reported in the literature for SIMdualKc applications to perennial crops, e.g., Paço et al. (2019) and Puig-Sirera et al. (2021) for olive, Darouich et al. (2022b) for clementine, Rosa (2018) for lemon, and Peddinti and Kambhammettu (2019) for orange. Thus, the obtained results may be considered appropriate for the analysis reported herein.

3.3. Assessing crop coefficients and crop water use

3.3.1. Almond orchards

For almond, the $K_{cb\ ini}$, $K_{cb\ mid}$, and $K_{cb\ end}$ were calibrated to 0.22, 0.58, and 0.50, respectively (Table 7). No differences were noticed between the two locations (P1 and P2), which were nearby. Trees were 5 years old (Table 1), thus corresponding to the mature stage in almond trees (Drechsler et al., 2022; López-López et al., 2018; García-Tejero et al., 2015). Mid-season f_c and h values of 0.41–0.42 and 4.0 m, respectively, and end-season f_c and h values of 0.20 and 4.0 m were observed (Table 5).

The calibrated $K_{cb\ mid}$ was close to the indicative value (0.60) tabulated by Pereira et al. (2021c), which correspond to a f_c of 0.40–0.50 and h of 4.0–5.0 m. The $K_{cb\ mid}$ was also close to the $K_{cb\ mid}$ of 0.60 reported by Espadafor et al. (2015) with 4 years old trees, f_c of 0.60, and h of 4.8 m. Likewise, López-López et al. (2018) reported $K_{cb\ mid}$ of 0.55 and 0.68 for 6 and 7 years old almond trees, with f_c of 0.55 and 0.59, respectively, and h of 4.8 m. In Sánchez et al. (2021), the low f_c of 0.41 observed corresponded to a small $K_{cb\ mid}$ of 0.36. However, Rallo et al. (2021) reported similar $K_{cb\ mid}$ for almond orchards with f_c of 0.40–0.50 and h of 4.0–5.0 m. These comparisons indicate that the orchards have a canopy and height smaller than expected for mature almonds orchard, which may be due to short trees spacing, heavy pruning, and less appropriate training. The previously referred salinity occurrence is nevertheless small and is not sufficient to justify the low development of the almond orchards, which likely also result from poor soil fertility. For the end-season, the calibrated $K_{cb\ end}$ (0.50) was higher than expected, e.g., the values (0.40) proposed by Rallo et al. (2021), and corresponding to f_c of 0.50–0.60 as tabulated by Pereira et al. (2021c). The calibrated $K_{cb\ end}$ was also higher than in Espadafor et al. (2015) and López-López et al. (2018). The large $K_{cb\ end}$ is likely due to irrigation applied much longer after harvesting which relates with the observed dryness of October-November.

Fig. 7 shows the dynamics of the potential (not stressed) basal crop coefficients (K_{cb}) in the two almond fields during both seasons. In P1, the large drop observed in the $K_{cb\ act}$ in 2019, which translates the reduction of the $T_{c\ act}$ relative to T_c, was likely explained by water and salinity stress, when measured EC_e was higher than the $EC_{e\ threshold}$. In the next year, 2020, no salinity stress occurred but the $K_{cb\ act}$ failed again to reach the potential K_{cb} values due to deficient irrigation scheduling during the dry summer season. Water stress in almond trees is reported to reduce vegetative growth and canopy size, also affecting the accumulation of reserves. During the growing season, water shortages during the kernel-filling stage may reduce nut weight and may affect fruit loads in the next season (López-López et al., 2018; Goldhamer and Girona, 2012). This likely occurred in P1 while in P2 the $K_{cb\ act}$ matched the K_{cb} values throughout both seasons, i.e., no water or salinity stresses were observed.

Fig. 7 further shows the dynamics of the soil evaporation coefficients (K_e) in both fields and seasons. The K_e could only be indirectly influenced by the salinity stress if f_c would be affected and consequently increase the soil surface exposure to solar radiation (Rosa et al., 2016). As salinity stress was only transient, likely resulting from some more intensive fertigation events rather than soil, groundwater, or irrigation water quality related causes, the f_c was apparently not affected. The dynamics of the K_e values were the same in both P1 and P2 fields, showing multiple high peaks during the rainfall seasons when the entire soil surface was wet ($f_w = 1$), and quite low values during the irrigation seasons when the resulting soil wetted fraction was small ($f_w \leq 0.12$) because of drip irrigation. The K_c curves, as well as the K_{cb} curves (Fig. 7), resulted similar to those for olives, with K_{cb} higher in spring-summer when transpiration is higher, and K_c high in fall and winter when rain occurs, and small in summer when rain is rare.

3.3.2. Olive orchards

The calibrated K_{cb} for each crop stage of olive varied only slightly in the three fields (P3, P4, and P5), with $K_{cb\ ini}$, $K_{cb\ mid}$, and $K_{cb\ end}$ assuming values of 0.32–0.33, 0.35–0.36, and 0.33–0.34, respectively (Table 7). Trees were 11–12 years old, with mid-season f_c and h values of 0.23–0.27 and 3.0–4.1 m, respectively, and end-season f_c and h values of 0.20–0.23 and 2.8–4.0 m, respectively (Table 5).

The calibrated $K_{cb\ mid}$ values were slightly lower than the indicative value (0.40) tabulated by Pereira et al. (2021c) for olive orchards with f_c of 0.35 and h of 3.5 m. They were also lower than the proposed value (0.40) in Rallo et al. (2021) for orchards with f_c of 0.20–0.30 and h of 3.0–3.5 m. Apparently, when compared with existing reviews, f_c and h values were expected to be larger, thus values now reported may be due

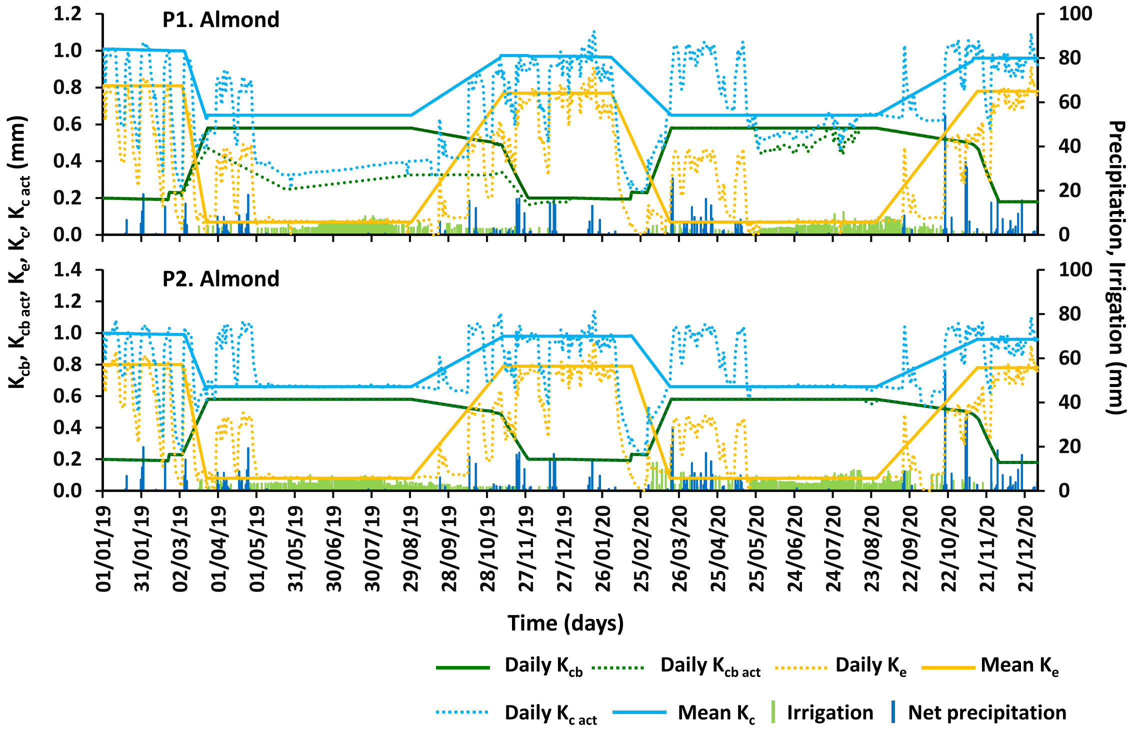

Fig. 7. Seasonal variation of the standard (non-stressed) basal crop coefficient (K_{cb}), the actual basal crop coefficient ($K_{cb\ act}$), the evaporation coefficient (K_e), and the actual crop coefficient ($K_{c\ act} = K_{cb\ act} + K_e$) in almond, P1 and P2, during the 2019–2020 growing seasons.

to excessive pruning and less good training. More adequate values were obtained when applying the Allen & Pereira (A&P) approach (Allen and Pereira, 2009; Pereira et al., 2020a, 2021c) using observed f_c and h values. On the other hand, the calibrated $K_{cb\ end}$ was consistent with the indicative values in Pereira et al. (2021c) and Rallo et al. (2021). Yet, the existing literature shows a wide range of variation of the K_{cb} in mature olive orchards, with calibrated $K_{cb\ mid}$ values approaching those in Villalobos et al. (2000) for a traditional orchard (cv. Picual) in southern Spain, with 278 trees ha^{-1}, $f_c = 0.3$ and h = 4.0, while the $K_{cb\ end}$ values were relatively higher, likely because irrigation in the study orchards was extended until the end of October/beginning of November. Differently, the calibrated $K_{cb\ mid}$ were lower while the $K_{cb\ end}$ approached the values reported in Puig-Sirera et al. (2021) for a traditional orchard in Sicily, Italy, with 250 trees ha^{-1}, $f_c = 0.35$, and h = 3.5. K_{cb} values in Conceição et al. (2017) and Santos (2018) were also comparable to those in this study. These authors estimated the K_{cb} of olive orchards with similar characteristics (trees 8–10 years old; 300 trees ha^{-1}; $f_c = 0.25$; h = 3.5–3.7 m) in the Alentejo region using sap-flow measurements.

The major contrast between olive and almond fields was in the dynamics of the $K_{cb\ act}$, with daily values in olive departing from the potential K_{cb} between May (all plots in 2019) and July (P5 in 2020), maintaining this condition up to the September (Fig. 8). This agreed with various reports available in the literature addressing the relationship between olive oil yields and water application, and confirming that oil yields are maximized at water application rates below 100% of full irrigation (Ahumada-Orellana et al., 2018; Hernández et al., 2018; Rosecrance et al., 2015; Ramos and Santos, 2010; Moriana et al., 2007, 2003; Grattan et al., 2006). Moderated water stress can also significantly reduce tree growth, thus reducing shoot growth, trunk growth, and pruning weights. These are however objectives for super intensive olive systems but, likely, too much stress has been imposed in the studied orchards which ended up limiting canopy development and f_c values. The dynamics of the K_e were similar to that in the almond fields. Higher K_e values were again noticed during winter when the entire soil surface was wetted, decreasing during the irrigation season as the wetted area reduced since drip irrigation was wetting the soil mostly under the canopies. The K_c curves (Fig. 8) are therefore similar to those reported by Paço et al. (2019) and Puig-Sirera et al. (2021).

3.3.3. Citrus orchards

The $K_{cb\ ini}$, $K_{cb\ mid}$, and $K_{cb\ end}$ for citrus were set to 0.40, 0.41, and 0.41, respectively, for the orange field (P6), and to 0.40, 0.40, and 0.40, respectively, for the clementine (P7) and mandarin (P8) fields (Table 7). Only minor differences were found between fields. Trees were 5 years old, with f_c varying from 0.25 to 0.29 along the growing seasons, and relatively short, with heights ranging from 2.4 m in P6 to 2.8 m in P8 (Table 5).

The calibrated K_{cb} values were comparable to those computed using the A&P approach (Allen and Pereira, 2009; Pereira et al., 2020a, 2021c) using the f_c and h values listed in Table 5 for the different crop stages. However, when compared to the indicative values in Pereira et al. (2021c) and Rallo et al. (2021), the calibrated $K_{cb\ mid}$ were found to be lower than those tabulated by for citrus orchards with f_c of 0.25–0.40 and h of 2.3–4.5 m. Citrus trees were thus likely trained small for easy harvesting which also resulted in small f_c. Closer values ($K_{cb} = 0.45$) were given in Allen and Pereira (2009) for citrus orchards with $f_{c\ eff}$ of 0.25, but with no ground cover, which was not the case in P6, P7, and P8. The calibrated K_{cb} values were also in close agreement with Villalobos et al. (2013) for 7 years old citrus trees, f_c of 0.27, and h equal to 2.30 m. The remaining dedicated literature was carried out in larger citrus trees, thus with larger f_c and h, showing consistently higher K_{cb} values (Darouich et al., 2022b; Jafari et al., 2021; Peddinti and Kambhammettu, 2019; Rallo et al., 2017; Taylor et al., 2017; Er-Raki et al., 2009).

In citrus fields (P6, P7, and P8), irrigation was characterized by large application depths, with seasonal values summing 548 mm (P6 in 2019) to 1170 mm (P8 in 2020 mm) (Table 3). These depths were more than enough to meet T_c values. As a result, no water stress was ever observed, with the $K_{cb\ act}$ matching always K_{cb} values in the three sites except when a slight salinity stress was noticed. This succeeded in P7 and P8 when the measured EC_e was above the $EC_{e\ threshold}$ of citrus for a short period (December 2019), causing the respective $K_{cb\ act}$ values to slightly

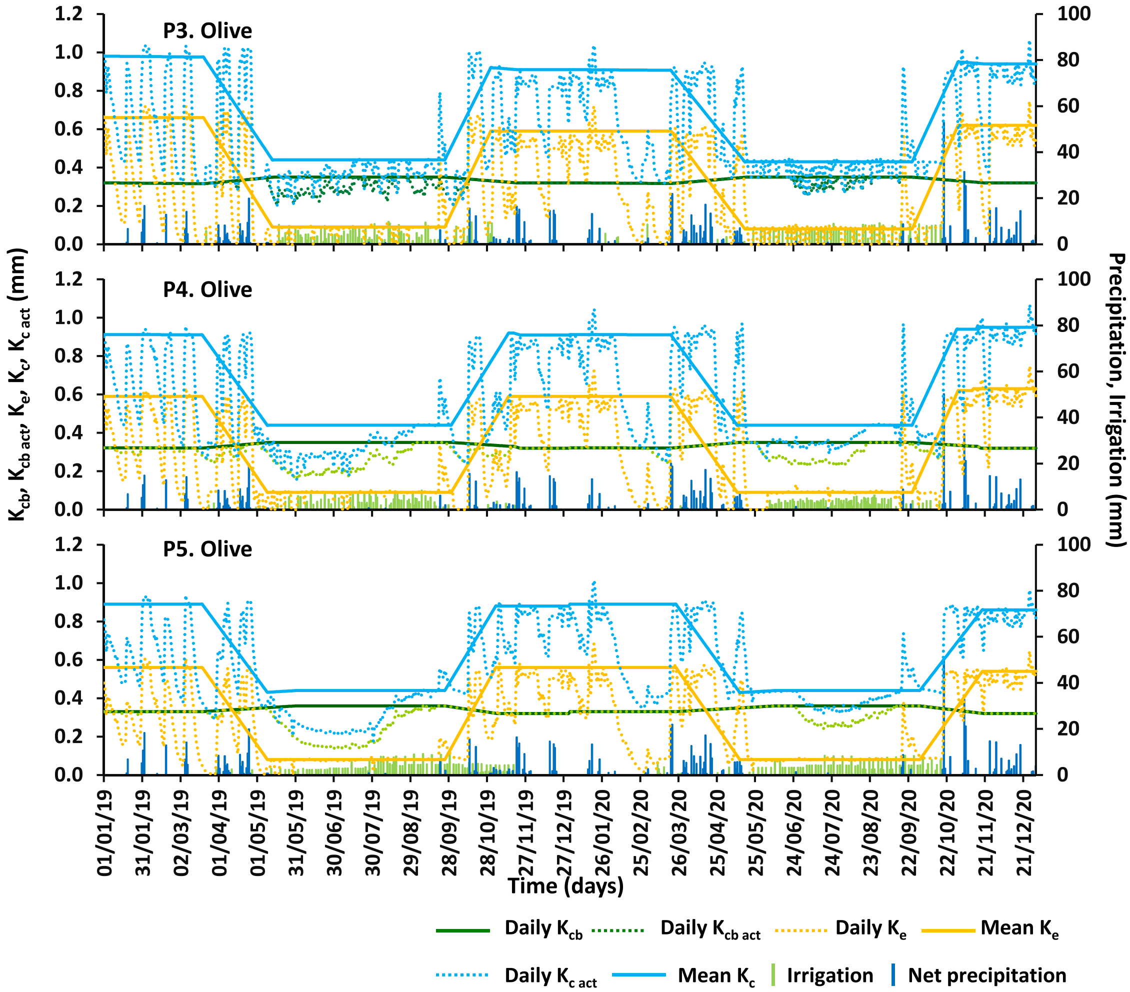

Fig. 8. Seasonal variation of the standard (non-stressed) basal crop coefficient (K_{cb}), the actual basal crop coefficient ($K_{cb\ act}$), the evaporation coefficient (K_e), and the actual crop coefficient ($K_{c\ act} = K_{cb\ act} + K_e$) in P3, P4, and P5 during the 2019–2020 growing seasons.

dropping from K_{cb} (Fig. 9). The dynamics of the K_e followed also the same trends reported above. Considering that rainfall occurs in fall and winter but not in summer, and that most of transpiration occurs in summer, it resulted that K_c curves are similar to those of olives. Differently, because citrus trees are active throughout the season if not heavy stressed, the K_{cb} curve has a constant value as already detected in a previous application with clementine (Darouich et al., 2022b).

3.3.4. Pomegranate

The $K_{cb\ ini}$, $K_{cb\ mid}$, and $K_{cb\ end}$ for pomegranate (P9) were calibrated to 0.24, 0.60, and 0.52, respectively (Table 7). Trees were also 5 years old, with mid-season f_c and h values of 0.41 and 2.5 m, and end-season f_c and h values of 0.30 and 2.3 m, respectively (Table 5). The calibrated $K_{cb\ mid}$ and $K_{cb\ end}$ were found to be higher than the indicative values in Rallo et al. (2021) for pomegranate orchards with f_c of 0.35–0.45 and h of 2.5–3.5 m. However, a better agreement was noticed between the calibrated $K_{cb\ mid}$ and the upper-class values given in Rallo et al. (2021), when f_c is above 0.45. Differently from the other crops, results for $K_{cb\ mid}$ fitted well those tabulated by Pereira et al. (2021c) but the $K_{cb\ end}$ was larger in the current study, which may be due to excess irrigation during the late season. $K_{cb\ mid}$ values reported by Niu et al. (2021) and Noory et al. (2021) likely were larger than in the current study but those authors did not provide for f_c values. Intrigliolo et al. (2021) reported also similar $K_{cb\ mid}$ but with a f_c of 0.58, which was much larger than the observed one.

Fig. 10 shows the $K_{cb\ act}$ always equaling K_{cb} values in the studied orchard despite high salinity EC_e values monitored in different dates along both growing seasons. As such, no water or salinity stress ever affected crop development. Nonetheless, research has shown that moderate water deficits during flowering and fruit set may increase aril red for some cultivars without detrimental effects on marketable yield, fruit size, and chemical composition. In addition, for some cultivars, during ripening and throughout the growing season, moderate water deficits may improve the red color of the fruit peel and/or juice but negatively affecting fruit weight and economic income (Volschenk, 2020; Martínez-Nicolás et al., 2019; Galindo et al., 2017; Intrigliolo et al., 2013). Yet, more research is needed for the Acco cultivar grown in P9. The K_c and K_{cb} curves (Fig. 10) are similar to those of almonds, also a deciduous tree, since transpiration and soil evaporation have contrary dynamics due to summer dryness.

3.4. Single crop coefficients as indicators of crop water use

Table 9 summarizes the mean K_c values computed from the sum of the computed $K_{cb\ act}$ and K_e during the crop stages of each case study using the SIMDualKc model. As already stated, the crop coefficients developed for different irrigation systems and different cultivars in different countries cannot be simply transferred to local management due to the complex characteristics of orchard systems, evidencing the necessity of conducting field research under local conditions (Rallo et al., 2021; Volschenk, 2020; Fereres et al., 2012). The K_c mean values depicted in Table 9 follow typical trends observed in drip systems as

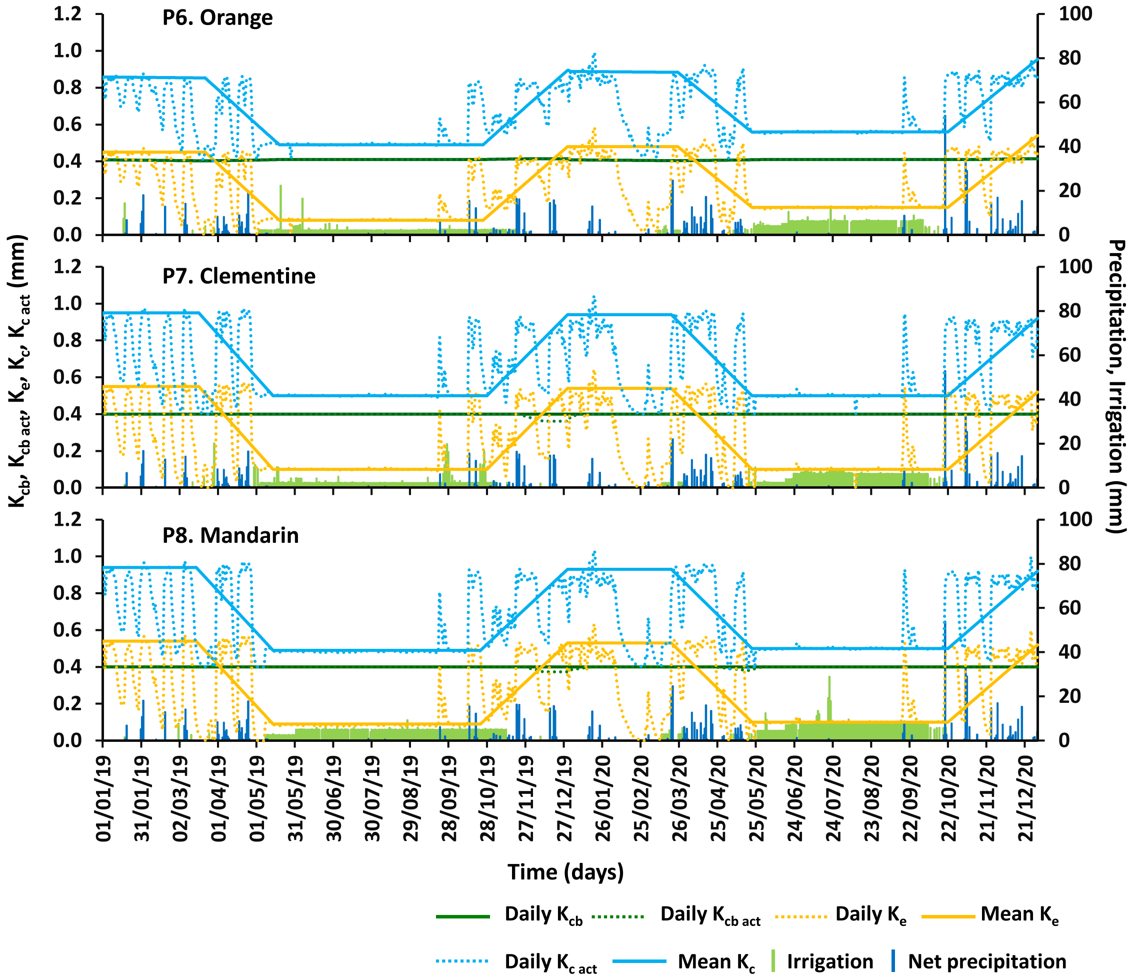

Fig. 9. Seasonal variation of the standard (non-stressed) basal crop coefficient (K_{cb}), the actual basal crop coefficient ($K_{cb\ act}$), the evaporation coefficient (K_e), and the actual crop coefficient ($K_{c\ act} = K_{cb\ act} + K_e$) in P6, P7, and P8 during the 2019–2020 growing seasons.

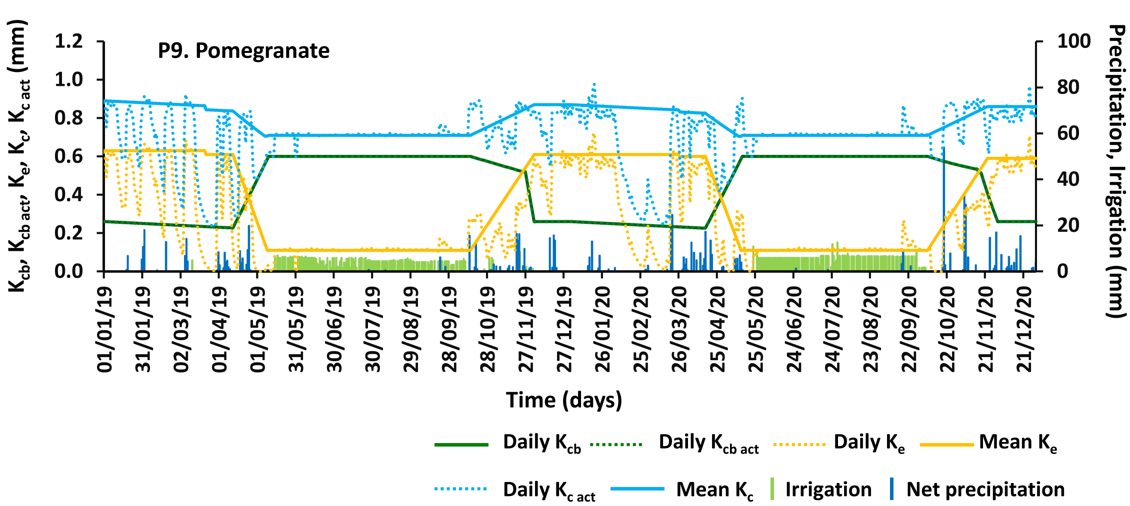

Fig. 10. Seasonal variation of the standard (non-stressed) basal crop coefficient (K_{cb}), the actual basal crop coefficient ($K_{cb\ act}$), the evaporation coefficient (K_e), and the actual crop coefficient ($K_{c\ act} = K_{cb\ act} + K_e$) in P9 during the 2019–2020 growing seasons.

already discussed in Darouich et al. (2022b) for citrus and Paço et al. (2019) for olive orchards. The K_{cb} curves (Figs. 7–10) result in FAO segmented curves with generally higher K_{cb} during the mid-season when irrigation is applied (spring and summer). Naturally, curves have smaller K_{cb} in the non-growing period, when transpiration is low, or much low, thus with the single K_c segmented curve showing a dynamic opposed to that of K_{cb} as discussed before relative to each crop. Because it also depends on soil evaporation, and thus on the fraction of the wetted soil surface, K_c (= $K_{cb} + K_e$) is smaller during the active growing period, when E_s and K_e are low due to negligeable precipitation and

Table 9
Mean crop coefficients (K_c) computed by SIMDualKc for the different crop stages and case studies.

Plot	Crop stages			
	Non-growing	Initial	Mid-season	End season
P1. Almond				
2019	1.01	1.00	0.65	0.97
2020	0.97	0.97	0.65	0.96
P2. Almond				
2019	1.00	0.99	0.66	0.96
2020	0.98	0.98	0.66	0.96
P3. Olive				
2019	0.98	0.98	0.44	0.92
2020	0.91	0.91	0.43	0.94
P4. Olive				
2019	0.91	0.91	0.44	0.92
2020	0.91	0.91	0.44	0.94
P5. Olive				
2019	0.89	0.89	0.44	0.88
2020	0.89	0.89	0.44	0.86
P6. Orange				
2019	0.86	0.85	0.49	0.89
2020	0.89	0.89	0.50	0.95
P7. Clementine				
2019	0.95	0.95	0.50	0.94
2020	0.94	0.94	0.50	0.92
P8. Mandarin				
2019	0.94	0.94	0.49	0.93
2020	0.93	0.93	0.50	0.92
P9. Pomegranate				
2019	0.88	0.84	0.71	0.84
2020	0.87	0.83	0.71	0.83

irrigation water applied directly along the trees' row, in small areas shaded by the canopies. Contrarily, K_c is larger in fall and winter (non-growing season, and initial and end-season crop stages), when rainfall occurs, and the entire soil surface contributes to soil evaporation.

The adequacy of the K_{cb} was already discussed in Section 3.3. In the analysis, it was evident that studies addressing the partition of the ET_c into its components are quite limited for some of the studied crops, namely almond and pomegranate. However, more information is available regarding the K_c values of these two crops. For almond, García-Tejero et al. (2018) provided a review of K_c values published in the literature, with many of their references reporting K_c values for the mid-season above 1.05. These values highly contrast with those in Table 9 and the tabulated values in Pereira et al. (2021c) and Rallo et al. (2021). Such differences can be attributed to several factors: (i) in those studies, irrigation was delivered through micro-sprinklers, thus increasing the K_e component in the K_c; (ii) most orchards were located in more fertile soils, with trees exhibiting larger canopies that resulted in higher transpiration rates and a larger weight of the K_{cb} component in K_c (Goldhamer and Fereres, 2017; Girona, 2006), while soils in P1 and P2 (Luvisols) are less fertile, with a very high fraction of coarse elements (> 70%); and (iii) yields in P1 and P2 were barely above 1.0 Mg ha^{-1} while several publications report yields ranging from 1.8 to 4.0 Mg ha^{-1} (López-López et al., 2018; Goldhamer and Fereres, 2017; Girona, 2006). Fruit load may also impact K_c and K_{cb} values in almonds as observed by López-López et al. (2018), who measured differences in the canopy conductance of trees with higher fruit load during the third year of observations, despite the same canopy size as the previous years.

For olive, $K_{c\ mid}$ values in Table 9 were comparable to those reported by Er-Raki et al. (2008) for an orchard in Morocco (fc=0.6; h=6.0) and by López-Olivari et al. (2016) in Chile (f_c=0.29–0.31; h=3.2 m). Yet, those orchards characteristics differed considerably from those in the Alentejo cases. For citrus, the $K_{c\ mid}$ values were in the range of values reported by Castel (2000), Consoli et al. (2006), and Er-Raki et al. (2009) for orchards with f_c ranging from 0.2 to 0.3. However, the $K_{c\ ini}$ and $K_{c\ end}$ differ considerably from the available literature. For pomegranate, the mean K_c values for the mid-season approached those in Intrigliolo et al. (2011) and Buesa et al. (2012) for southern Spain but were below those in Ayars et al. (2017) for California.

Hence, Table 9 includes K_c values adequate for irrigation water management of orchards in the Alentejo region of southern Portugal. The approach adopted combines information provided by soil water content measurements and simulated with the state-of-the-art SIMDualKc model to overcome the limitations of data collection and the impact of the three-dimensionality of drip irrigation on soil measurements. It is one of the most widely used methods for measuring crop evapotranspiration as reported in Pereira et al. (2020b) and Allen et al. (2011), being validated against other methodologies, namely sap-flow (Paço et al., 2019, 2014; Puig-Sirera et al., 2020). Still, the proposed K_c values need to be used with care, with proper consideration of the specific characteristics of local orchards.

3.5. Evaluation of the soil water balance in the studied orchards

3.5.1. Almond

Table 10 presents the soil water balance computed by SIMDualKc for the almond orchards (P1 and P2) during the 2019 and 2020 growing seasons. Seasonal net irrigation depths ranged from 596 to 772 mm, with less water applied always in P1 than in P2, particularly in 2020. Seasonal T_c values were naturally equal or very close in both fields, corresponding to 72.8–74.5% of the ET_c (880–907 mm). However, $T_{c\ act}$ values were remarkably different. In P1, $T_{c\ act}$ values were always below the potential T_c values, amounting to 377 and 613 mm in 2019 and 2020, respectively. In P2, $T_{c\ act}$ values practically matched the potential T_c values during both seasons (660–655 mm). Seasonal soil evaporation ranged from 224 to 237 mm, corresponding to 25.5–27.2% of the ET_c, and 26.6–38.1% of the $ET_{c\ act}$ (609–837 mm in P1; 907–892 mm in P2).

While seasonal $ET_{c\ act}$ values depend on tree age and size, climate conditions, interrow management, and irrigation methods, in P2, where no stress was observed, $ET_{c\ act}$ values were within the range of values reported in the literature for mature almond orchards. They were comparable to the $ET_{c\ act}$ values of 946 mm for a mature almond orchard (7 years old) with 7.3 m × 7.3 m tree spacing in Arbuckle, California, USA, in the early 1980 s (Fereres et al., 1982). Yet, they were far below more recent records, which refer to the need of 1250 mm for fully satisfying mature almond trees' water needs and reaching maximum yields in the southern San Joaquin Valley of California, USA (Goldhamer and Fereres, 2017).

Seasonal percolation differed also between fields. In P1, the impact of the salinity stress on transpiration rates resulted in an increase in percolation losses in the drier season of 2019 compared to 2020. As shown in Fig. 11, in that year, most of the estimated percolation values occurred during the irrigation season (about 73%) because of the osmotic stress impact on root water uptake. Obviously, the percolated water could have helped leach salts away from the rootzone, thus decreasing the impact of the salinity stress on crop transpiration. This cannot be simulated in SIMDualKc, except by providing inputs of the EC_e in the rootzone throughout the crop growing season. However, field measurements of the EC_e in 2019 were always higher than the crop tolerance salinity threshold. In 2020, percolation resulted mostly from rainfall. Also noticeable was that about 10% and 36% of percolation losses occurred in the late season stage of 2019 and 2020 seasons, respectively, because of late irrigation events often combined with rainfall depths above the soil's water holding capacity. In P2, higher percolation values were found, as expected, in the 2020 rainier season, when also some losses from irrigation events were noticed. Likely, the farmer of P1 adopted a more adequate irrigation schedule.

3.5.2. Olive

Soil water dynamics in olive fields (P3, P4, and P5) were remarkably different than in the almonds' cases. Seasonal irrigation depths were smaller, ranging from 266 to 357 mm (Table 10). Seasonal T_c values

Table 10
Components of the soil water balance.

Plot	I (mm)	P (mm)	ΔSW (mm)	T_c (mm)	$T_{c\ act}$ (mm)	E_s (mm)	DP (mm)	RO (mm)
P1. Almond								
2019	617	337	-9	661	377	232	323	6
2020	596	484	-10	656	613	224	207	24
P2. Almond								
2019	649	337	10	660	660	247	80	6
2020	772	484	5	656	655	237	316	20
P3. Olive								
2019	339	337	-24	431	378	195	73	10
2020	355	484	-13	427	410	204	174	38
P4. Olive								
2019	273	337	-52	433	339	200	9	18
2020	266	484	-39	428	374	226	60	50
P5. Olive								
2019	357	337	-52	445	340	192	100	14
2020	330	484	-15	440	404	215	136	47
P6. Orange								
2019	548	337	-8	516	516	180	177	27
2020	843	484	-8	510	510	258	526	27
P7. Clementine								
2019	653	337	8	505	504	213	252	14
2020	858	484	-18	499	499	214	580	38
P8. Mandarin								
2019	906	337	-3	505	504	199	517	8
2020	1170	484	-17	499	498	220	899	27
P9. Pomegranate								
2019	654	337	-22	649	649	219	84	6
2020	694	484	-21	637	637	222	268	26

Note: I, irrigation; P, precipitation; ΔSW, soil water storage variation; T_c, potential crop transpiration; $T_{c\ act}$, actual crop transpiration; E_s, soil evaporation; DP, deep percolation; RO, runoff.

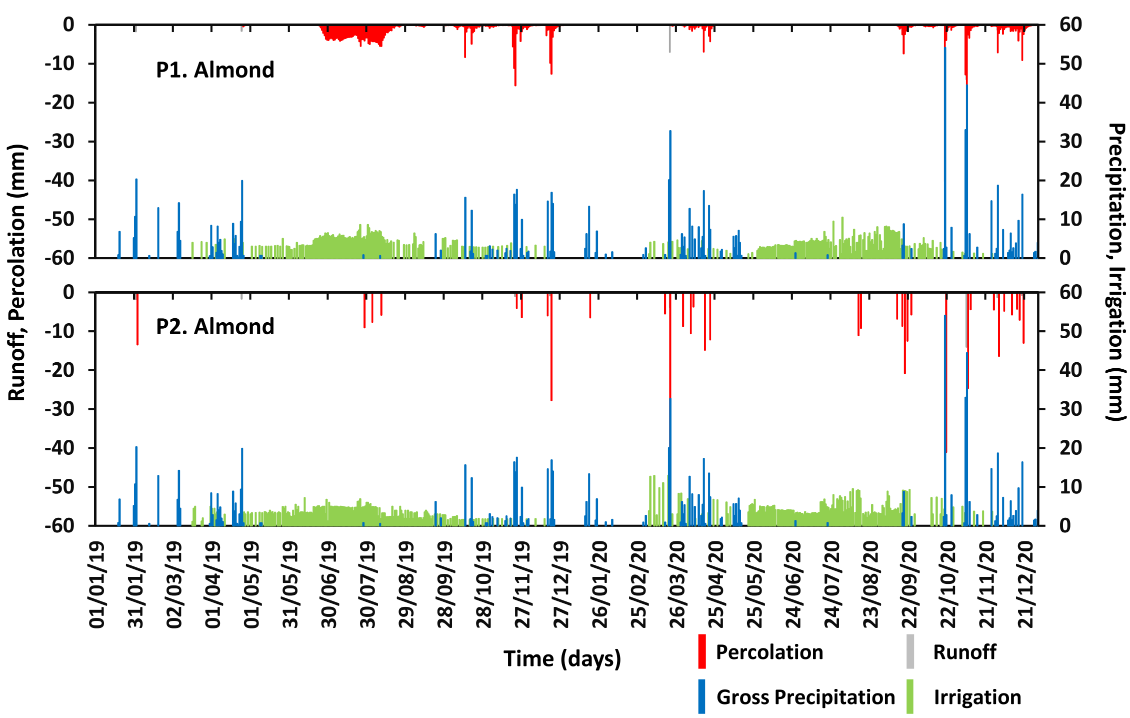

Fig. 11. Daily values of percolation and runoff in P1 and P2 during the 2019–2020 growing seasons.

were also lower than for almonds, summing 427–445 mm during both growing seasons (65.4–69.9% of the ET_c), which evidence the lower water requirements of olives compared to almonds. Differences between olive plots were related to planting densities and lengths of crop stages of the different varieties. The major contrast between olive and almond fields was in the dynamics of the $T_{c\ act}$ (and $K_{cb\ act}$) as discussed in Section 3.3.2. T_c reductions due to water stress ended up varying from 4.0% (P3 in 2020) to 23.6% (P5 in 2019). No salinity stress was ever registered, with the monitored EC_e always below the crop's salinity tolerance threshold. Seasonal soil evaporation ranged from 192 to 226 mm, corresponding to 30.1–34.6% of the ET_c (626–655 mm) and 33.2–37.7% of the $ET_{c\ act}$ (532–619 mm). The weight of soil evaporation on crop evapotranspiration was thus slightly higher than in the almond fields. Runoff (10–50 mm) and percolation (9–174 mm) resulted mostly

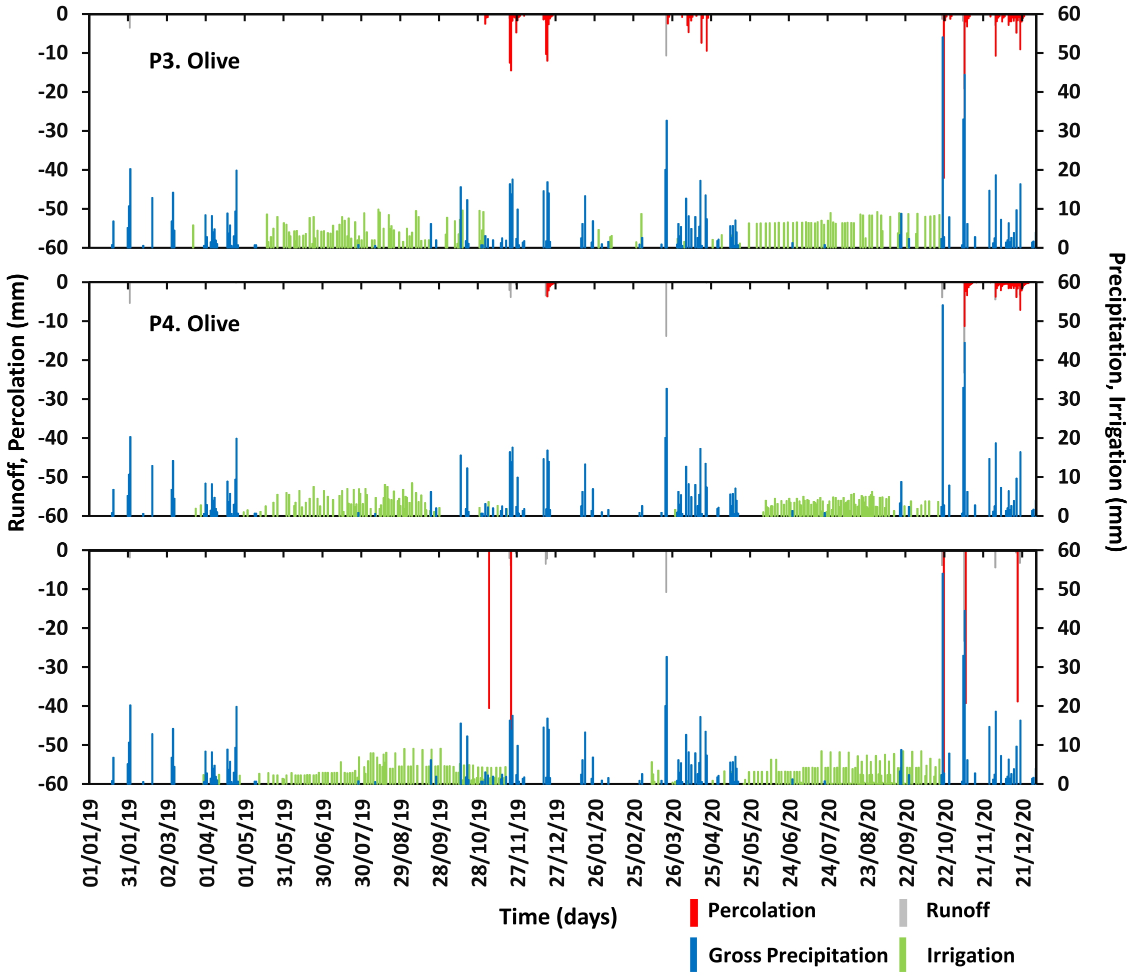

Fig. 12. Daily values of percolation and runoff in P3, P4, and P5 during the 2019–2020 growing seasons.

from rainfall events (Fig. 12). It is likely that olive farmers skills are better since irrigation of olives is practiced for a longer time than in almonds.

3.5.3. Citrus

In citrus fields (P6, P7, and P8), irrigation was characterized by large application depths, with seasonal values summing from 548 mm (P6 in 2019) to 1170 mm (P8 in 2020 mm) (Table 10). These depths were more than enough to meet T_c values, which only ranged from 499 (P7 in 2020) to 516 mm (P6 in 2019), corresponding to 66.4–74.1% of the ET_c. No water stress was ever observed while the salinity stress was only minor and affecting P7 and P8 for a very short period (December 2019; Fig. 9). Seasonal soil evaporation ranged from 180 to 258 mm, corresponding to 25.9–33.6% of the ET_c.

Deep percolation had a large weight compared to the other outputs of the soil water balance. The large percolation values, which the SIMDualKc estimated to range from 177 to 526 mm in the orange field (P6) to 517–899 mm in the mandarin field (P8), confirmed the excess water application. Contrarily to observations in almond and olive orchards, the percolation in citrus fields mainly occurred during the irrigation season (Fig. 13), when 66.0% (P6 in 2020) to 84.4% (P8 in 2020) of the seasonal percolation amounts were computed. It also corresponded to 32.3% (P6 in 2019) to 76.8% (P8 in 2020) of the total irrigation water applied.

The results of the water balance in the citrus fields have obviously no other justification than complete mismanagement of irrigation water. It is known that citrus trees can endure mild-moderate water stress except for the most critical growth stages, which are the flowering and fruit growth periods (García-Tejero et al., 2012). For this reason, deficit irrigation practices have long been evaluated in the main citrus production areas due to limited water resource availability (Pagán et al., 2022, Rallo et al, 2017; Ballester et al., 2011; García Tejero et al., 2011). Better management practices need thus to be implemented in the three commercial orchards.

3.5.4. Pomegranate

Pomegranate is far less studied than the crops above, which highlights the importance of the respective monitoring (P9). The seasonal irrigation depth reached 654 mm in 2019 and 694 mm in 2020 (Table 10). These values are below the 848 and 932 mm applied by surface drip in trees of similar age of the cultivar 'Wonderful' in California (Ayars et al., 2017). Their totals are also within the range of depths (392–776 mm) reported for cultivars 'Mollar de Elche' and 'Wonderful' (7–13 years old) grown in soils with different textures in southern Spain as reviewed by Volschenk (2020).

Seasonal T_c values amounted 649 (2019) and 637 mm (2020), corresponding respectively to 74.8% and 74.2% of the ET_c. These seasonal values were lower than those reported in Ayars et al. (2017) for trees of the same age (912–953 mm) grown in California. No water or salinity stresses were noticed in the pomegranate orchard, even if the monitored EC_e values were in general the highest of all cases. Seasonal soil evaporation corresponded to 25.2% (219 mm) and 25.8% (222 mm) of the ET_c in 2019 and 2020, respectively. More significant percolation was computed in 2020, with approximately 37% of the seasonal amount occurring during the irrigation season, which corresponded to 39% of the water applied (Fig. 14). Thus, despite better than for citrus, there is

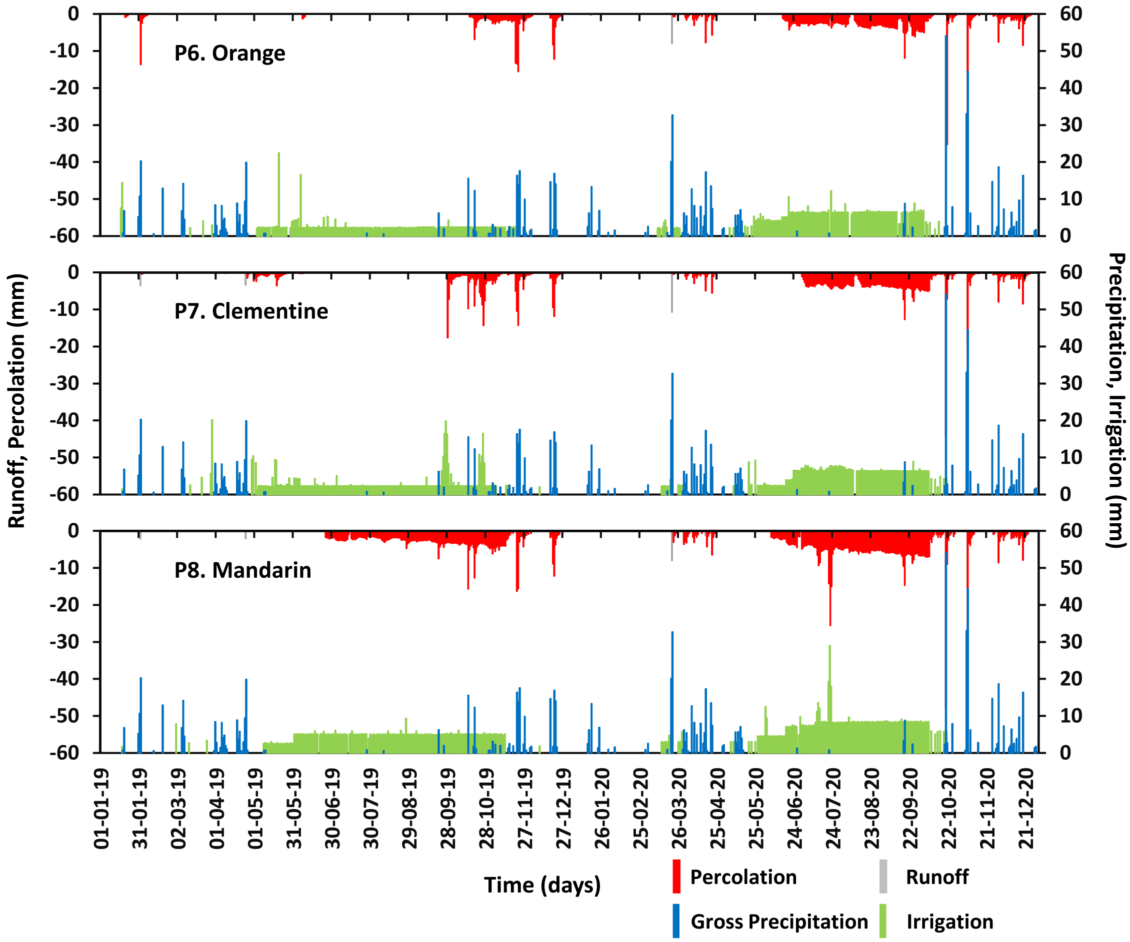

Fig. 13. Daily values of percolation and runoff in P6, P7, and P8 during the 2019–2020 growing seasons.

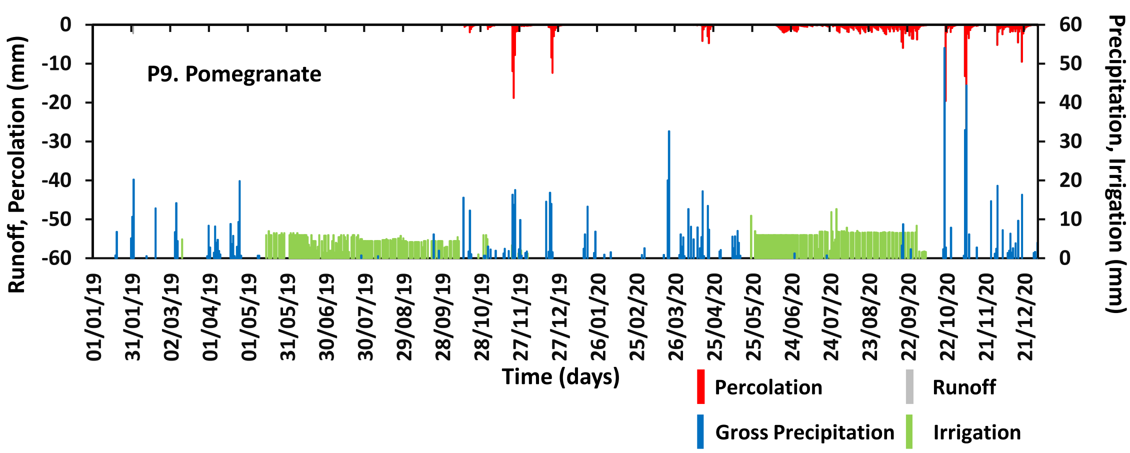

Fig. 14. Daily values of percolation and runoff in P9 during the 2019–2020 growing seasons.

room for improvement and water saving.

3.6. Searching improved water use with SIMDualKc

Fig. 15 exemplifies the evolution of the $K_{cb\ act}$, K_e, and $K_{c\ act}$ in selected plots (P1, P5, P8, and P9) when considering a mild deficit irrigation scheduling scenario. The soil water balance is then presented for all plots in Table 11. The mild deficit scenario included the same dates of the crop stages in each growing season as well as the previously calibrated model parameters. Irrigation triggering was set for a Management Allowable Depletion (MAD) of 1.05 θ_p, while irrigation depths were set to 5 mm following the observed data in Table 3. No salinity effects were considered due to its transient nature.

Table 11 shows a reduction of the $T_{c\ act}$ values of 3.0% (P5, P7, and P8 in 2020) to 5.2% (P1 in 2019) relative to the T_c values, thus with no effect on crop yields considering the tolerance of the study crops to mild water deficits as explained above. Percolation estimates returned the greatest contrast when compared with the farmers schedules, with reductions reaching 63–98% in the almond fields, 17–58% in the olive fields, 82–100% in the citrus fields, and 70–98% in the pomegranate

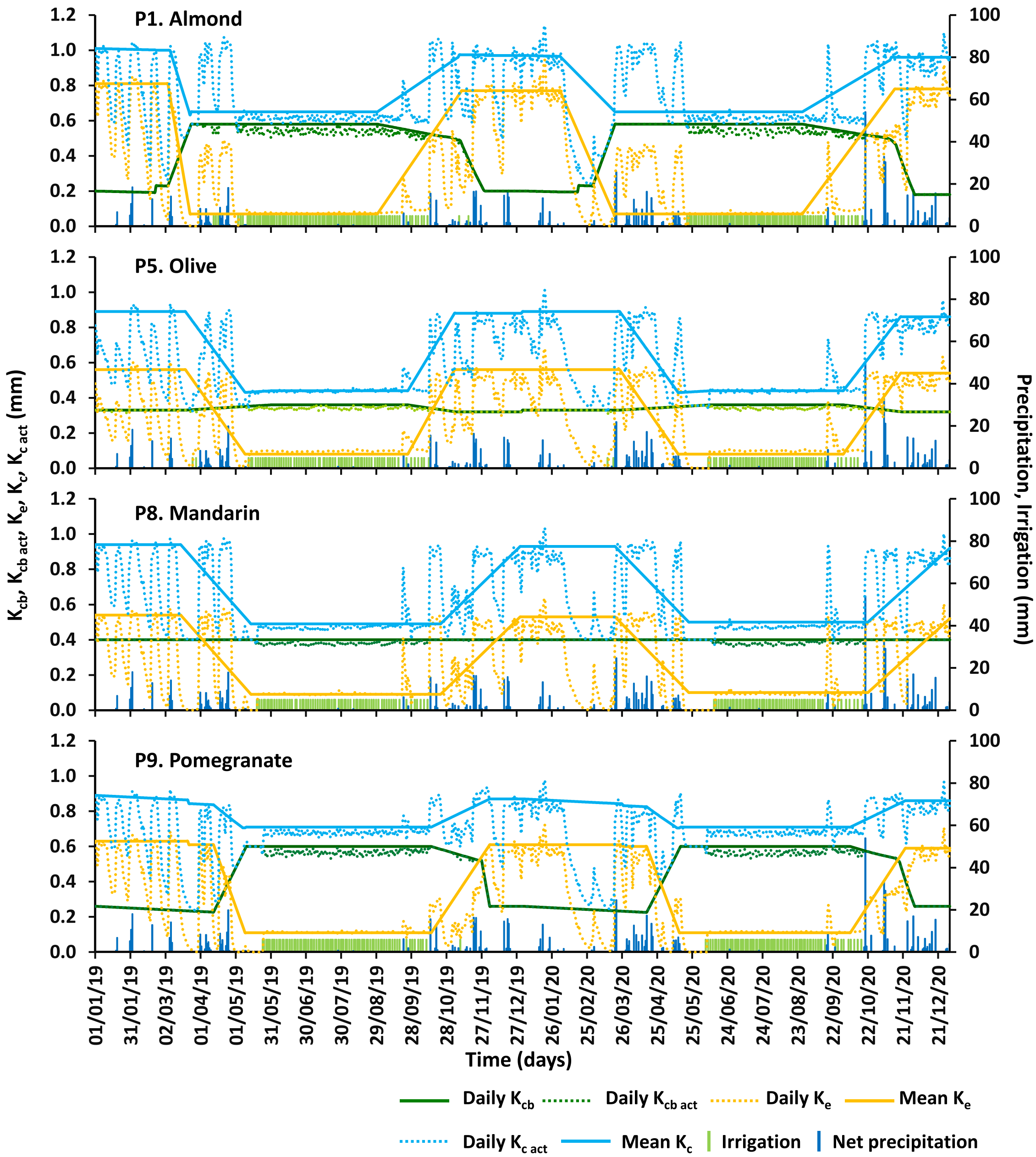

Fig. 15. Seasonal variation of the standard (non-stressed) basal crop coefficient (K_{cb}), the actual basal crop coefficient ($K_{cb\ act}$), the evaporation coefficient (K_e), and the actual crop coefficient ($K_{c\ act} = K_{cb\ act} + K_e$) in P1, P5, P8 and P9 when considering a mild irrigation scheduling scenario.

field. This confirms that most of percolation losses were due to poor irrigation scheduling. All other components of the water balance showed similar estimates as those obtained when analysing the farmers schedules. As such, the mild deficit irrigation scheduling scenario shows possible water savings of 20 mm in case of olives, up to 855 mm for citrus. Yet, for olive, water savings were naturally only possible when the observed water stress was less pronounced than the one considered in the modeling scenario.

4. Conclusions

The current paper presents and discusses estimates of crop evapotranspiration in nine commercial orchards in the Alentejo region of southern Portugal. The crops addressed were almonds, olive, citrus (orange, clementine, and mandarin), and pomegranate. In all case studies, crop evapotranspiration was estimated by computing the soil water balance following the FAO56 dual-K_c approach adopted in the SIMDualKc model, i.e., through the partition of crop evapotranspiration into its components, crop transpiration, and soil evaporation. The model may be considered one of the most adequate solutions for computing the water balance in such complex agricultural systems; it is able to estimate the K_{cb} at various crop stages taking into consideration the crop density through a density coefficient K_d, which is a function of f_c and h. In addition, it accounts for the effects of interrow management (active ground cover and mulching, namely dried understory plants and falling leaves) and soil conditions (mainly soil salinity) on actual transpiration rates. The model successfully simulated the soil water contents measured in the different fields along two growing seasons, with root mean square error values lower than 0.005 $m^3\ m^{-3}$ and modeling efficiencies from 0.363 to 0.782.

For almonds, differences to the literature were noticed, especially for the K_c and when compared to almond orchards from California, which

Table 11
Water savings considering a mild deficit irrigation scheduling scenario.

Plot	Farmers I (mm)	Mild deficit scenario I (mm)	P (mm)	ΔSW (mm)	T_c (mm)	$T_{c\ act}$ (mm)	E_s (mm)	DP (mm)	RO (mm)	WS (%)
P1. Almond										
2019	617	535	337	-17	661	626	220	6	5	13.3
2020	596	475	484	-13	656	626	216	77	31	20.3
P2. Almond										
2019	649	535	337	11	660	627	228	24	6	17.6
2020	772	480	484	5	656	627	221	77	20	37.8
P3. Olive										
2019	339	365	337	-24	431	416	215	38	10	-
2020	355	335	484	-13	427	412	221	134	38	5.6
P4. Olive										
2019	273	375	337	-51	433	418	219	8	18	-
2020	266	330	484	-39	428	414	238	71	50	-
P5. Olive										
2019	357	370	337	-19	445	429	207	42	13	-
2020	330	310	484	-15	440	427	214	94	46	6.1
P6. Orange										
2019	548	355	337	-7	516	499	170	11	6	35.2
2020	843	330	484	-4	510	494	191	94	26	60.9
P7. Clementine										
2019	653	360	337	-6	505	490	186	3	14	44.9
2020	858	315	484	-8	499	484	191	74	38	63.3
P8. Mandarin										
2019	906	365	337	-13	505	488	194	1	8	59.7
2020	1170	315	484	-8	499	484	196	81	27	73.1
P9. Pomegranate										
2019	654	510	337	-17	649	621	210	1	6	22.0
2020	694	474	484	-17	637	610	215	82	26	31.7

Note: I, irrigation; P, precipitation; ΔSW, soil water storage variation; T_c, potential crop transpiration; $T_{c\ act}$, actual crop transpiration; E_s, soil evaporation; DP, deep percolation; RO, runoff; WS, water saving.

were mainly attributed to the irrigation management, soil fertility, fruit load, training, and crop height and canopy size. Salinity levels in one of the fields during the 2019 growing season led to significant water uptake reductions, resulting most likely from intensive fertigation mismanagement. For olive, small differences in the K_{cb} and K_c values were noticed between the three case studies, which were related to the fraction of the ground covered by the trees' canopies and height. Mild water stress conditions were noticed in the three monitored fields, generally corresponding to a water saving strategy with no impact on oil yields. In citrus fields, the estimated K_{cb} and K_c values were relatively small when compared with the existing literature, which was justified by orchards' training. Monitoring of irrigation practices in the three case studies showed a large excess irrigation water application, with translated into large percolation losses. Lastly, for pomegranate, information on the partition of the ET_c was quite limited and, as far as we know, this is one of the first studies assessing separately the dynamics of the K_{cb} and K_e in this crop. Like in the citrus fields, excess application of irrigation water was observed, but without the same magnitude of losses estimated for the clementine and mandarin fields.

This study provides more accurate K_c values for the orchard systems in the Roxo Irrigation District, thus also providing for improving irrigation water management in the Alentejo region. A proper characterization of evapotranspiration fluxes and dynamics was needed for further studies, namely the assessment of soil salinization and nutrient leaching risks resulting from current agricultural practices. With these aims, data and parameterization obtained in this study were used with the calibrated model SIMDualKc to develop alternative irrigation management issues, mainly improved schedules. Results show a potential water saving of 82–292 mm for almond, 20 mm for olive, 193–855 mm for citrus, particularly for mandarin, and 144–220 mm for pomegranate. However, modeling tools are insufficient for improving irrigation and it is desirable that farmers are trained, including in their computing skills, and that support on the various orchard management issues, namely relative to water and fertility, become available, thus contributing to better facing global change challenges.

Declaration of Competing Interest

The authors declare that they have no known competing financial interests or personal relationships that could have appeared to influence the work reported in this paper.

Data Availability

Data will be made available on request.

Acknowledgments

This research project was funded by Fundação para a Ciência e Tecnologia (FCT), Portugal, through project SOIL4EVER (PTDC/ASP-SOL/28796/2017). The support of FCT through grants attributed to T. B. Ramos (CEECIND/01152/2017) and H. Darouich (CEECIND/01153/2017) is acknowledged.

References

Ahumada-Orellana, L.E., Ortega-Farías, S., Searles, P.S., 2018. Olive oil quality response to irrigation cut-off strategies in super high-density orchard. Agric. Water Manag. 202, 81–88. https://doi.org/10.1016/j.agwat.2018.02.008.

Alexandre, C., Borralho, T., Durão, A., 2018. Evaluation of salinization and sodification in irrigated areas with limited soil data: case study in southern Portugal. Span. J. Soil Sci. 8, 102–120. https://doi.org/10.3232/SJSS.2018.V8.N1.07.

Allen, R.G., Pereira, L.S., 2009. Estimating crop coefficients from fraction of ground cover and height. Irrig. Sci. 28, 17–34. https://doi.org/10.1007/s00271-009-0182-z.

Allen, R.G., Pereira, L.S., Raes, D., Smith, M., 1998. Crop Evapotranspiration. Guidelines for Computing Crop Water Requirements, FAO Irrig. Drain. Paper 56. FAO, Rome, Italy, 300 pp.

Allen, R.G., Pereira, L.S., Smith, M., Raes, D., Wright, J.L., 2005. FAO-56 dual crop coefficient method for estimating evaporation from soil and application extensions. J. Irrig. Drain. Eng. 131 (1), 2–13. https://doi.org/10.1061/(ASCE)0733-9437(2005)131:1(2).

Allen, R.G., Wright, J.L., Pruitt, W.O., Pereira, L.S., Jensen, M.E., 2007. Water requirements. In: Hoffman, G.J., Evans, R.G., Jensen, M.E., Martin, D.L., Elliot, R.L. (Eds.), Design and Operation of Farm Irrigation Systems, 2nd edition. ASABE, St. Joseph, MI, pp. 208–288.

Allen, R.G., Pereira, L.S., Howell, T.A., Jensen, M.E., 2011. Evapotranspiration information reporting: I. Factors governing measurement accuracy. Agric. Water Manag. 98 (6), 899–920. https://doi.org/10.1016/j.agwat.2010.12.015.

Ayars, J.E., Phene, C.J., Phene, R.C., Gao, S., Wang, D., Day, K.R., Makus, D.J., 2017. Determining pomegranate water and nitrogen requirements with drip irrigation. Agric. Water Manag. 187, 11–23. https://doi.org/10.1016/j.agwat.2017.03.007.

Ayers, R.S., Westcot, D.W., 1985. Water Quality for Agriculture. Irrig. Drain. Paper 29. FAO, Rome, p. 174.

Ballester, C., Castel, J., Introgliolo, D.S., Castel, J.R., 2011. Response of Clementina de Nules citrus trees to summer deficit irrigation. Yield components and fruit composition. Agric. Water Manag. 98, 1027–1032. https://doi.org/10.1016/j.agwat.2011.01.011.

Bellvert, J., Adeline, K., Baram, S., Pierce, L., Sanden, B.L., Smart, D.R., 2018. Monitoring crop evapotranspiration and crop coefficients over an almond and pistachio orchard throughout remote sensing. Remote Sens 10, 2001. https://doi.org/10.3390/rs10122001.

Buesa, I., Badal, E., Guerra, D., García, J., Lozoya, A., Bartual, J., Intrigliolo, D.S., Bonet, L., 2012. Development of an irrigation scheduling recommendation for pomegranate trees (Punica granatum). II International Symposium on the Pomegranate. Options Méditerranéennes 103, 141–145.

Cameira, M.R., Pereira, A., Ahuja, L., Ma, L., 2014. Sustainability and environmental assessment of fertigation in an intensive olive grove under Mediterranean conditions. Agric. Water Manag. 146, 346–360. https://doi.org/10.1016/j.agwat.2014.09.007.

Cancela, J.J., Fandiño, M., Rey, B.J., Martinez, E.M., 2015. Automatic irrigation system based on dual crop coefficient, soil and plant water status for Vitis vinifera (cv Godello and cv Mencía. Agric. Water Manag. 151, 52–63. https://doi.org/10.1016/j.agwat.2014.10.020.

Castel, R.J., 2000. Water use of developing citrus canopies in Valencia, Spain. In: Proc. Int. Soc. Citriculture, IX Congr. Florida, USA, 2000. pp. 223–226.

Chen, N., Li, X., Šimůnek, J., Shi, H., Hu, Q., Zhang, Y., Xin, M., 2022. Evaluating soil salt dynamics under biodegradable film mulching with different disintegration rates in an arid region with shallow and saline groundwater: Experimental and modeling study. Geoderma 423, 115969. https://doi.org/10.1016/j.geoderma.2022.115969.

Conceição, N., Tezza, L., Häusler, M., Lourenço, S., Pacheco, C.A., Ferreira, M.I., 2017. Three years of monitoring evapotranspiration components and crop and stress coefficients in a deficit irrigated intensive olive orchard. Agric. Water Manag. 191, 138–152. https://doi.org/10.1016/j.agwat.2017.05.011.

Consoli, S., O'Connell, N., Snyder, R., 2006. Estimation of evapotranspiration of different-sized navel-orange tree orchards using energy balance. J. Irrig. Drain. Eng. 132, 2–8. https://doi.org/10.1061/(ASCE)0733-9437(2006)132:1(2).

Coops, N., Loughhead, A., Ryan, P., Hutton, R., 2001. Development of daily spatial heat unit mapping from monthly climatic surfaces for the Australian continent. Int. J. Geogr. Inf. Syst. 15, 345–361. https://doi.org/10.1080/13658810010011401.

Dane, J.H., Hopmans, J.W., 2002. Pressure plate extractor. In: Dane, J.H., Topp, G.C. (Eds.), Methods of Soil Analysis, Part 4, Physical Methods. Soil Science Society of America Book Series, Soil Science Society of America, Madison, Wisconsin, pp. 688–690.

Darouich, H., Ramos, T.B., Pereira, L.S., Rabino, D., Bagagiolo, G., Capello, G., Simionesei, L., Cavallo, E., Biddoccu, M., 2022a. Water use and soil water balance of mediterranean vineyards under rainfed and drip irrigation management: evapotranspiration partition and soil management modelling for resource conservation. Water 14, 554. https://doi.org/10.3390/w14040554.

Darouich, H., Karfoul, R., Ramos, T.B., Moustafa, A., Pereira, L.S., 2022b. Searching for sustainable-irrigation issues of clementine orchards in the Syrian Akkar Plain: Effects of irrigation method and canopy size on crop coefficients, transpiration, and water use with SIMDualKc model. Water 14, 2052. https://doi.org/10.3390/w14132052.

Degrandi-Hoffman, G., Thorp, R., Loper, G., Eisikowitch, D., 1996. Describing the progression of almond bloom using accumulated heat units. J. Appl. Ecol. 33, 812–818. https://doi.org/10.2307/2404951.

DGADR, 2021. Aproveitamento hidroagrícolas do Grupo II no Continente. Culturas e áreas regadas em 2020. Direcção Geral de Agricultura e do Desenvolvimento Rural, Ministério da Agricultura e Alimentação, Lisboa, Portugal.

Dinheiro Vivo, 2021. 〈https://www.dinheirovivo.pt/economia/nacional/zero-mas-praticas-no-olival-nascido-do-alqueva-sao-regra-e-nao-excecao-13478423.html〉 (Last accessed 13.07.2022).

Doorenbos, J., Kassam, A.H., 1979. Yield Response to Water. In: FAO Irrigation and Drainage Paper 33. FAO, Rome, 193 pp.

Drechsler, K., Fulton, A., Kisekka, I., 2022. Crop coefficients and water use of young almond orchards. Irrig. Sci. 40, 379–395. https://doi.org/10.1007/s00271-022-00786-y.

EDIA, 2022. Empresa de Desenvolvimento e Infraestruturas do Alqueva. Beja, Portugal. 〈http://www.edia.pt/en/〉 (Last accessed 12.07.2022).

Egea, J., Ortega, E., Martínez-Gómez, P., Dicenta, F., 2003. Chilling and heat requirements of almond cultivars for flowering. Environ. Exp. Bot. 50, 79–85. https://doi.org/10.1016/S0098-8472(03)00002-9.

Er-Raki, S., Chehbouni, A., Hoedjes, J., Ezzahar, J., Duchemin, B., Jacob, F., 2008. Improvement of FAO-56 method for olive orchards through sequential assimilation of thermal infrared based estimates of ET. Agric. Water Manag. 95, 309–321. https://doi.org/10.1016/j.agwat.2007.10.013.

Er-Raki, S., Chehbouni, A., Guemouria, N., Ezzahar, J., Khabba, S., Boulet, G., Hanich, L., 2009. Citrus orchard evapotranspiration: Comparison between eddy covariance measurements and the FAO-56 approach estimates. Plant Biosyst. 143, 201–208. https://doi.org/10.1080/11263500802709897.

Espadafor, M., Orgaz, F., Testi, L., Lorite, I.J., Villalobos, F.J., 2015. Transpiration of young almond trees in relation to intercepted radiation. Irrig. Sci. 33, 265–275. https://doi.org/10.1007/s00271-015-0464-6.

Expresso, 2018 〈https://expresso.pt/economia/2018–10-01-Governo-garante-que-o-olival-intensivo-nao-cria-pressoes-ambientais-no-Alentejo〉 (Last accessed 13.07.2022).

Fandiño, M., Cancela, J.J., Rey, B.J., Martínez, E.M., Rosa, R.G., Pereira, L., 2012. Using the dual-K_c approach to model evapotranspiration of Albariño vineyards (Vitis vinifera L. cv. Albariño) with consideration of active ground cover. Agric. Water Manag. 112, 75–87. https://doi.org/10.1016/j.agwat.2012.06.008.

Fereres, E., Martinich, D.A., Aldrich, T.M., Castel, J.R., Holzapfel, E., Schulbach, H., 1982. Drip irrigation saves money in young almond orchards. Calif. Agric. 36, 12–13.

Fereres, E., Goldhamer, D., Sadras, V., Smith, M., Marsal, J., Girona, J., Naor, A., Gucci, R., Caliandro, A., Ruz, C., 2012. Yield response to water of fruit trees and vines: guidelines. In: Steduto, P., Hsiao, T., Fereres, E., Raes, D. (Eds.), Crop yield response to water. FAO Irrigation and Drainage Paper Nº. 66. Food and Agriculture Organization of the United Nations, Rome.

Galindo, A., Calín-Sánchez, A., Griñán, I., Rodríguez, P., Cruz, Z.N., Girón, I.F., Corell, M., Martínez-Font, R., Moriana, A., Carbonell-Barrachina, A.A., Torrecillas, A., Hernández, F., 2017. Water stress at the end of the pomegranate fruit ripening stage produces earlier harvest and improves fruit quality. Sci. Hortic. 226, 68–74. https://doi.org/10.1016/j.scienta.2017.08.029.

García Tejero, I., Durán Zuazo, V.H., Jiménez Bocanegra, J.A., Muriel Fernández, J.L., 2011. Improved water-use efficiency by deficit irrigation programmes: Implications for saving water in citrus orchards. Sci. Hort. 128, 274–282. https://doi.org/10.1016/j.scienta.2011.01.035.

García-Tejero, I., Romero-Vicente, R., Jiménez-Bocanegra, J.A., Martínez-García, G., Durán-Zuazo, V.H., Muriel-Fernández, J.L., 2010. Response of citrus trees to deficit irrigation during different phenological periods in relation to yield, fruit quality, and water productivity. Agric. Water Manag. 97, 689–699. https://doi.org/10.1016/j.agwat.2009.12.012.

García-Tejero, I., Durán-Zuazo, V.H., Arriaga-Sevilla, J., Muriel Fernández, J.L., 2012. Impact of water stress on citrus yield. Agron. Sustain. Dev. 32, 651–659. https://doi.org/10.1007/s13593-011-0060-y.

García-Tejero, I., Moriana, A., Rodríguez Pleguezuelo, C.R., Durán Zuazo, V.H., Egea, G., 2018. Sustainable deficit-irrigation management in almonds (Prunus dulcis L.): different strategies to assess the crop water use. Chapter 12. In: García-Tejero, I.F., Durán Zuazo, V.H. (Eds.), Water Scarcity and Sustainable Agriculture in Semiarid Environment. Academic Press, pp. 271–298. https://doi.org/10.1016/B978-0-12-813164-0.00012-0. Chapter 12.

García-Tejero, I.F., Hernández, A., Rodríguez, V.M., Ponce, J.R., Ramos, V., Muriel, J.L., Durán-Zuazo, V.H., 2015. Estimating almond crop coefficients and physiological response to water stress in semiarid environments (SW Spain). J. Agric. Sci. Technol. 17, 1255–1266.

Garrido, A., Fernández-González, M., Álvarez-López, S., González-Fernández, E., Rodríguez-Rajo, F.J., 2020. First phenological and aerobiological assessment of olive orchards at the Northern limit of the Mediterranean bioclimatic area. Aerobiologia 36, 641–656. https://doi.org/10.1007/s10453-020-09659-3.

Garrido, A., Fernández-González, M., Vázquez-Ruiz, R.A., Rodríguez-Rajo, F.J., Aira, M.J., 2021. reproductive biology of olive trees (Arbequina cultivar) at the northern limit of their distribution areas. Forests 12, 204. https://doi.org/10.3390/f12020204.

Girona, J., 2006. La respuesta del cultivo del almendro al riego. Vida Rural 234, 12–16.

Goldhamer, D.A., Fereres, E., 2017. Establishing an almond water production function for California using long-term yield response to variable irrigation. Irrig. Sci. 35, 169–179. https://doi.org/10.1007/s00271-016-0528-2.

Goldhamer, D.A., Girona, J., 2012. Almond. In: Steduto, P., Hsiao, T.C., Fereres, E., Raes, D. (Eds.), Crop yield response to water. FAO Irrigation and Drainage Paper Nº. 66. Food and Agriculture Organization of the United Nations, Rome, pp. 358–373.

González, M.G., Ramos, T.B., Carlesso, R., Paredes, P., Petry, M.T., Martins, J.D., Aires, N.P., Pereira, L.S., 2015. Modelling soil water dynamics of full and deficit drip irrigated maize cultivated under a rain shelter. Biosyst. Eng. 132, 1–18. https://doi.org/10.1016/j.biosystemseng.2015.02.001.

González-Altozano, P., Castel, J.R., 2000. Regulated deficit irrigation in 'Clementina de Nules' citrus trees. II: Vegetative growth. J. Hortic. Sci. Biotechnol. 75, 388–392. https://doi.org/10.1080/14620316.2000.11511256.

Grattan, S.R., Berenguer, M.J., Connell, J.H., Polito, V.S., Vossen, P.M., 2006. Olive oil production as influenced by different quantities of applied water. Agric. Water Manag. 85, 133–140. https://doi.org/10.1016/j.agwat.2006.04.001.

Hernández, M.L., Velásquez-Palmero, D., Sicardo, M.D., Fernández, J.E., Diaz-Espejo, A., Martínez-Rivas, J.M., 2018. Effect of a regulated deficit irrigation strategy in a hedgerow 'Arbequina' olive orchard on the mesocarp fatty acid composition and desaturase gene expression with respect to olive oil quality. Agric. Water Manag. 204, 100–106. https://doi.org/10.1016/j.agwat.2018.04.002.

Hersbach, H., Bell, B., Berrisford, P., Biavati, G., Horányi, A., Muñoz Sabater, J., Nicolas, J., Peubey, C., Radu, R., Rozum, I., Schepers, D., Simmons, A., Soci, C., Dee, D., Thépaut, J.-N., 2018. ERA5 hourly data on single levels from 1979 to present. Copernicus Climate Change Service (C3S) Climate Data Store (CDS). 〈https://doi.org/10.24381/cds.adbb2d47〉 (Last accessed 04-01-2022).

Intrigliolo, D.S., Nicolas, E., Bonet, L., Ferrer, P., Alarcón, J.J., Bartual, J., 2011. Water relations of field grown Pomegranate trees (Punica granatum) under different drip irrigation regimes. Agric. Water Manag. 98, 691–696. https://doi.org/10.1016/j.agwat.2010.11.006.

Intrigliolo, D.S., Bonet, L., Nortes, P.A., Puerto, H., Nicolas, E., Bartual, J., 2013. Pomegranate trees performance under sustained and regulated deficit irrigation. Irrig. Sci. 31 (5), 959–970. https://doi.org/10.1007/s00271-012-0372-y.

Intrigliolo, D.S., Wang, D., Pérez-Gago, M.B., Palou, L., Ayars, J., Puerto, H., Bartual, J., 2021. Water requirements and responses to irrigation restrictions. In: Sarkhosh, A., Yavari, A.M., Zamani, Z. (Eds.), The pomegranate: botany, production and uses. CAB International, p.p. 320–343.

IUSS Working Group WRB, 2014. World Reference Base for Soil Resources 2014. International Soil Classification System for Naming Soils and Creating Legends for Soil Maps. World Soil Resources Reports No. 106. FAO, Rome.

Jafari, M., Kamali, H., Keshavarz, A., Momeni, A., 2021. Estimation of evapotranspiration and crop coefficient of drip-irrigated orange trees under a semi-arid climate. Agric. Water Manag. 248, 106769 https://doi.org/10.1016/j.agwat.2021.106769.

Jovanovic, N., Pereira, L.S., Paredes, P., Pôças, I., Cantore, V., Todorovic, M., 2020. A review of strategies, methods and technologies to reduce non-beneficial consumptive water use on farms considering the FAO56 methods. Agric. Water Manag. 239, 106267 https://doi.org/10.1016/j.agwat.2020.106267.

Kool, D., Agam, N., Lazarovitch, N., Heitman, J.L., Sauer, T.J., Ben-Gal, A., 2014. A review of approaches for evapotranspiration partitioning. Agric. Meteorol. 184, 56–70. https://doi.org/10.1016/j.agrformet.2013.09.003.

Legates, D., McCabe, G., 1999. Evaluating the use of goodness of fit measures in hydrologic and hydroclimatic model validation. Water Resour. Res. 35, 233–241. https://doi.org/10.1029/1998WR900018.

Liu, M., Shi, H., Paredes, P., Ramos, T.B., Dai, L., Feng, Z., Pereira, L.S., 2022a. Estimating and partitioning maize evapotranspiration as affected by salinity using weighing lysimeters and the SIMDualKc model. region. Agric. Water Manag. 261, 107362 https://doi.org/10.1016/j.agwat.2021.107362.

Liu, M., Paredes, P., Shi, H., Ramos, T.B., Dou, X., Dai, L., Pereira, L.S., 2022b. Impacts of a shallow saline water table on maize evapotranspiration and groundwater contribution using static water table lysimeters and the dual Kc water balance model SIMDualKc. Agric. Water Manag. 273, 107887 https://doi.org/10.1016/j.agwat.2022.107887.

Liu, Y., Pereira, L.S., Fernando, R.M., 2006. Fluxes through the bottom boundary of the root zone in silty soils: Parametric approaches to estimate groundwater contribution and percolation. Agric. Water Manag. 84, 27–40. https://doi.org/10.1016/j.agwat.2006.01.018.

López-López, M., Espadafor, M., Testi, L., Lorite, I.J., Orgaz, F., Fereres, E., 2018. Water requirements of mature almond trees in response to atmospheric demand. Irrig. Sci. 36, 271–280. https://doi.org/10.1007/s00271-018-0582-z.

López-Olivari, R., Ortega-Farías, S., Poblete-Echeverría, C., 2016. Partitioning of net radiation and evapotranspiration over a superintensive drip-irrigated olive orchard. Irrig. Sci. 34, 17–31. https://doi.org/10.1007/s00271-015-0484-2.

López-Urrea, R., de Santa Olalla, Martín, Montoro, F., López-Fuster, P, A., 2009. Single and dual crop coefficients and water requirements for onion (Allium cepa L.) under semiarid conditions. Agric. Water Manag. 96 (6), 1031–1036. https://doi.org/10.1016/j.agwat.2009.02.004.

Luo, Q., 2011. Temperature thresholds and crop producTion: A Review. Clim. Chang. 109, 583–598. https://doi.org/10.1007/s10584-011-0028-6.

Martínez-Nicolás, J.J., Galindo, A., Griñána, I., Rodríguez, P., Cruze, Z.N., Martínez-Fonta, R., Carbonell-Barrachinaf, A.A., Nourig, H., Melgarejoa, P., 2019. Irrigation water saving during pomegranate flowering and fruit set period do not affect Wonderful and Mollar de Elche cultivars yield and fruit composition. Agric. Water Manag. 226, 1–7. https://doi.org/10.1016/j.agwat.2019.105781.

Martins, J.C., Vilar, M.T., Neves, M.J., Pires, F.P., Ramos, T.B., Prazeres, A.O., Gonçalves, M.C., 2005. Monitorização da salinidade e sodicidade de solos regados por rampas rotativas nos perímetros do Roxo e de Odivelas. Proceedings of the I National Congress of Irrigation and Drainage (CD-ROM), 5 to 8 of December. Centro Operativo e de Tecnologia do Regadio, Beja, Portugal.

Melgarejo, P., Martínez-Valero, R., Guillamón, J.M., Miró, M., Amarós, A., 1997. Phenological stages of the pomegranate tree (*Punka granatum* L.). Ann. Appl. Biol. 130, 135–140. https://doi.org/10.1111/j.1744-7348.1997.tb05789.x.

Melo-Abreu, J.P., Barranco, D., Cordeiro, A.M., Tous, J., Rogado, B.M., Villalobos, F.J., 2004. Modelling olive flowering date using chilling for dormancy release and thermal time. Agric. Meteorol. 125, 117–127. https://doi.org/10.1016/j.agrformet.2004.02.009.

Minhas, P.S., Ramos, T.B., Ben-Gal, A., Pereira, L.S., 2020. Coping with salinity in irrigated agriculture: crop evapotranspiration and water management issues. Agric. Water Manag. 227, 105832 https://doi.org/10.1016/j.agwat.2019.105832.

Moriana, A., Orgaz, F., Fereres, E., Pastor, M., 2003. Yield responses of a mature olive orchard to water deficits. J. Am. Soc. Hort. Sci. 128, 425–431. https://doi.org/10.21273/JASHS.128.3.0425.

Moriana, A., Pérez-López, D., Gómez-Rico, A., Salvador, M., Olmedilla, N., Riba, F., Fregapane, G., 2007. Irrigation scheduling for traditional, low-density olive orchards: water relations and influence on oil characteristics. Agric. Water Manag. 87, 1171–1179. https://doi.org/10.1016/j.agwat.2006.06.017.

Moriasi, D.N., Arnold, J.G., Van Liew, M.W., Bingner, R.L., Harmel, R.D., Veith, T.L., 2007. Model evaluation guidelines for systematic quantification of accuracy in watershed simulations. Trans. ASABE 50, 885–900. https://doi.org/10.13031/2013.23153.

Nash, J.E., Sutcliffe, J.V., 1970. River flow forecasting through conceptual models part I—a discussion of principles. J. Hydrol. 10, 282–290. https://doi.org/10.1016/0022-1694(70)90255-6.

Nelson, D.W., Sommers, L.E., 1982. Total carbon, organic carbon, and organic matter. In: Page, A.L., et al. (Eds.), Methods of Soil Analysis. Part 2. Chemical and Microbiological Properties. Agron. Monogr. 9. ASA and SSSA, Madison, WI, pp. 539–579.

Niu, H., Zhao, T., Wei, J., Wang, D., Chen, Y., 2021. Reliable tree-level evapotranspiration estimation of pomegranate trees using lysimeter and UAV multispectral imagery. IEEE Conference on Technologies for Sustainability (SusTech), Irvine, CA, USA, pp. 1–6. ⟨https://doi.org/10.1109/SusTech51236.2021.9467413⟩.

Noory, H., Abbasnejad, M., Ebrahimian, H., Azadi, H., 2021. Determining evapotranspiration and crop coefficients of young and mature pomegranate trees under drip irrigation. Irrig. Drain. 70, 1073–1084. https://doi.org/10.1002/ird.2607.

Paço, T.A., Ferreira, M.I., Rosa, R.D., Paredes, P., Rodrigues, G.C., Conceição, N., Pacheco, C.A., Pereira, L.S., 2012. The dual crop coefficient approach using a density factor to simulate the evapotranspiration of a peach orchard: SIMDualKc model versus eddy covariance measurements. Irrig. Sci. 30, 115–126. https://doi.org/10.1007/s00271-011-0267-3.

Paço, T.A., Pôças, I., Cunha, M., Silvestre, J.C., Santos, F.L., Paredes, P., Pereira, L.S., 2014. Evapotranspiration and crop coefficients for a super intensive olive orchard. An application of SIMDualKc and METRIC models using ground and satellite observations. J. Hydrol. 519, 2067–2080. https://doi.org/10.1016/j.jhydrol.2014.09.075.

Paço, T.A., Paredes, P., Pereira, L.S., Silvestre, J., Santos, F.L., 2019. Crop coefficients and transpiration of a super intensive Arbequina olive orchard using the dual K_c approach and the K_{cb} computation with the fraction of ground cover and height. Water 11, 383. https://doi.org/10.3390/w11020383.

Pagán, E., Robles, J.M., Temnani, A., Berríos, P., Botía, P., Pérez-Pastor, A., 2022. Effects of water deficit and salinity stress on late mandarin trees. Sci. Total Environ. 803, 150109 https://doi.org/10.1016/j.scitotenv.2021.150109.

Peddinti, S.R., Kambhammettu, B.V.N.P., 2019. Dynamics of crop coefficients for citrus orchards of central India using water balance and eddy covariance flux partition techniques. Agric. Water Manag. 212, 68–77. https://doi.org/10.1016/j.agwat.2018.08.027.

Pereira, L.S., Oweis, T., Zairi, A., 2002. Irrigation management under water scarcity. Agric. Water Manag. 57, 175–206. https://doi.org/10.1016/S0378-3774(02)00075-6.

Pereira, L.S., Gonçalves, J.M., Dong, B., Mao, Z., Fang, S.X., 2007. Assessing basin irrigation and scheduling strategies for saving irrigation water and controlling salinity in the upper Yellow River Basin, China. Agric. Water Manag. 93, 109–122. https://doi.org/10.1016/j.agwat.2007.07.004.

Pereira, L.S., Cordery, I., Iacovides, I., 2009. Coping with Water scarcity. Addressing the Challenges. Springer, Dordrecht, p. 382.

Pereira, L.S., Allen, R.G., Smith, M., Raes, D., 2015a. Crop evapotranspiration estimation with FAO56: Past and future. Agric. Water Manag. 147, 4–20. https://doi.org/10.1016/j.agwat.2014.07.031.

Pereira, L.S., Paredes, P., Rodrigues, G.C., Neves, M., 2015b. Modeling malt barley water use and evapotranspiration partitioning in two contrasting rainfall years. Assessing AquaCrop and SIMDualKc models. Agric. Water Manag. 159, 239–254. https://doi.org/10.1016/j.agwat.2015.06.006.

Pereira, L.S., Paredes, P., Melton, F., Johnson, L., Wang, T., López-Urrea, R., Cancela, J. J., Allen, R., 2020a. Prediction of crop coefficients from fraction of ground cover and height. Background and validation using ground and remote sensing data. Agric. Water Manag. 241, 106197 https://doi.org/10.1016/j.agwat.2020.106197.

Pereira, L.S., Paredes, P., Jovanovic, N., 2020b. Soil water balance models for determining crop water and irrigation requirements and irrigation scheduling focusing on the FAO56 method and the dual K_c approach. Agric. Water Manag. 241, 106357 https://doi.org/10.1016/j.agwat.2020.106357.

Pereira, L.S., Paredes, P., López-Urrea, R., Hunsaker, D.J., Mota, M., Mohammadi Shad, Z., 2021a. Standard single and basal crop coefficients for vegetable crops, an update of FAO56 crop water requirements approach. Agric. Water Manag. 241, 106197 https://doi.org/10.1016/j.agwat.2020.106196.

Pereira, L.S., Paredes, P., Hunsaker, D.J., López-Urrea, R., Mohammadi Shad, Z., 2021b. Standard single and basal crop coefficients for field crops. Updates and advances to the FAO56 crop water requirements method. Agric. Water Manag. 243, 106466 https://doi.org/10.1016/j.agwat.2020.106466.

Pereira, L.S., Paredes, P., Melton, F., Johnson, L., Mota, M., Wang, T., 2021c. Prediction of crop coefficients from fraction of ground cover and height: Practical application to vegetable, field, and fruit crops with focus on parameterization. Agric. Water Manag. 2021 (252), 106663 https://doi.org/10.1016/j.agwat.2020.106663.

Phogat, V., Skewes, M.A., McCarthy, M.G., Cox, J.W., Šimůnek, J., Petrie, P., 2017. Evaluation of crop coefficients, water productivity, and water balance components for wine grapes irrigated at different deficit levels by a sub-surface drip. Agric. Water Manag. 180, 22–34. https://doi.org/10.1016/j.agwat.2016.10.016.

Portela, M.M., Espinosa, L.A., Zelenakova, M., 2020. Long-term rainfall trends and their variability in mainland Portugal in the last 106 years. Climate 8, 146. https://doi.org/10.3390/cli8120146.

Publico, 2021. ⟨https://www.publico.pt/2021/11/24/p3/fotogaleria/oil-dorado-retrato-alentejo-desfigurado-monoculturas-intensivas-407130⟩ (Last accessed 13.07.2022).

Puig-Sirera, À., Rallo, G., Paredes, P., Paço, T.A., Minacapilli, M., Provenzano, G., Pereira, L.S., 2021. Transpiration and water use of an irrigated traditional olive grove with sap-flow observations and the FAO56 dual crop coefficient approach. Water 13, 2466. https://doi.org/10.3390/w13182466.

Rallo, G., González-Altozano, P., Manzano-Juárez, J., Provenzano, G., 2017. Using field measurements and FAO-56 model to assess the eco-physiological response of citrus orchards under regulated deficit irrigation. Agric. Water Manag. 180, 136–147. https://doi.org/10.1016/j.agwat.2016.11.011.

Rallo, G., Paço, T.A., Paredes, P., Puig-Sirera, À., Massai, R., Provenzano, G., Pereira, L. S., 2021. Updated single and dual crop coefficients for tree and vine fruit crops. Agric. Water Manag. 250, 106645 https://doi.org/10.1016/j.agwat.2020.106645.
Ramos, A.F., Santos, F.L., 2010. Yield and olive oil characteristics of a low-density orchard (cv. Cordovil) subjected to different irrigation regimes. Agric. Water Manag. 97 (2), 363–373. https://doi.org/10.1016/j.agwat.2009.10.008.
Ramos, T.B., Šimůnek, J., Gonçalves, M.C., Martins, J.C., Prazeres, A., Pereira, L.S., 2012. Two-dimensional modeling of water and nitrogen fate from sweet sorghum irrigated with fresh and blended saline waters. Agric. Water Manag. 111, 87–104. https://doi.org/10.1016/j.agwat.2012.05.007.
Ramos, T.B., Darouich, H., Šimůnek, J., Gonçalves, M.C., Martins, J.C., 2019. Soil salinization in very high-density olive orchards grown in southern Portugal: current risks and possible trends. Agric. Water Manag. 217, 265–281. https://doi.org/10.1016/j.agwat.2019.02.047.
Ritchie, J.T., 1972. Model for predicting evaporation from a row crop with incomplete cover. Water Resour. Res. 8, 1204–1213. https://doi.org/10.1029/WR008i005p01204.
Romano, N., Hopmans, J.W., Dane, J.H., 2002. Suction table. In: Dane, J.H., Topp, G.C. (Eds.), Methods of Soil Analysis, Part 4, Physical Methods. Soil Science Society of America Book Series, Soil Science Society of America, Madison, Wisconsin, pp. 692–698.
Rosa, R.D., 2018. Modelação da evapotranspiração com o modelo SIMDualKc: Aplicação à rega de fruteiras, a consociações de culturas e a condições salinas, e ligação ao SIG para análise à escala do projeto de rega. Instituto Superior de Agronomia, Lisboa, Portugal, 292 p.
Rosa, R.D., Paredes, P., Rodrigues, G.C., Alves, I., Allen, R.G., Pereira, L.S., 2012. Implementing the dual crop coefficient approach in interactive software. 1. Background and computational strategy. Agric. Water Manag. 103, 8–24. https://doi.org/10.1016/j.agwat.2011.10.013.
Rosa, R.D., Ramos, T.B., Pereira, L.S., 2016. The dual Kc approach to assess maize and sweet sorghum transpiration and soil evaporation under saline conditions: Application of the SIMDualKc model. Agric. Water Manag. 103, 77–94. https://doi.org/10.1016/j.agwat.2016.06.028.
Rosecrance, R.C., Krueger, W.H., Milliron, L., Bloese, J., Garcia, C., Mori, B., 2015. Moderate regulated deficit irrigation can increase olive oil yields and decrease tree growth in super high density 'Arbequina' olive orchards. Sci. Hort. 190, 75–82. https://doi.org/10.1016/j.scienta.2015.03.045.
Sánchez, J.M., Simón, L., González-Piqueras, J., Montoya, F., López-Urrea, R., 2021. Monitoring crop evapotranspiration and transpiration/evaporation partitioning in a drip-irrigated young almond orchard applying a two-source surface energy balance model. Water 13, 73. https://doi.org/10.3390/w13152073.
Santos, F.L., 2018. Olive water use, crop coefficients, yield, and water productivity under two deficit irrigation strategies. Agronomy 8, 89. https://doi.org/10.3390/agronomy8060089.
Sanz-Cortés, F., Martinez-Calvo, J., Badenes, M.L., Bleiholder, H., Hack, H., Llacer, G., Meier, U., 2002. Phenological growth stages of olive trees (Olea europaea). Ann. Appl. Biol. 140, 151–157. https://doi.org/10.1111/j.1744-7348.2002.tb00167.x.
Silva, S.P., Valín, M.I., Mendes, S., Araujo-Paredes, C., Cancela, J., 2021. Dual crop coefficient approach in Vitis vinifera L. cv. Loureiro. Agronomy 11, 2062. https://doi.org/10.3390/agronomy11102062.
SNIRH, 2022. Serviço Nacional de Informação dos Recursos Hídricos. Agência Portuguesa do Ambiente, Lisboa, Portugal. ⟨https://snirh.apambiente.pt/⟩ (Last accessed 13–07-2022).
Stewart, J.I., Hagan, R.M., Pruitt, W.O., Danielson, R.E., Franklin, W.T., Hanks, R.J., Riley, J.P., Jackson, E.B., 1977. Optimizing Crop Production through Control of Water and Salinity Levels in the Soil. Utah Water Research Laboratory, Reports Paper 67, Logan, 191 pp.
Taylor, N.J., Annandale, J.G., Vahrmeijer, J.T., Ibraimo, N.A., Mahohoma, W., Gush, M. B., Allen, R.G., 2017. Modelling water use of subtropical fruit crops: the challenges. Acta Hortic. 1160, 277–284. https://doi.org/10.17660/ActaHortic.2017.1160.40.
UNESCO, 2020. United Nations World Water Development Report 2020. Water and Climate Change, Paris, UNESCO.
USDA-SCS, 1972. National Engineering Handbook, Section 4, Table 10.1. Washington, DC.
Villalobos, F.J., Orgaz, F., Testi, L., Fereres, E., 2000. Measurement and modeling of evapotranspiration of olive (Olea europaea L,). Eur. J. Agron. 13, 155–163. https://doi.org/10.1016/S1161-0301(00)00071-X.
Villalobos, F.J., Testi, L., Orgaz, F., García-Tejera, O., Lopez-Bernal, A., González-Dugo, M.V., Ballester-Lurbe, C., Castel, J.R., Alarcón-Cabañero, J.J., Nicolás-Nicolás, E., Girona, J., Marsal, J., Fereres, E., 2013. Modelling canopy conductance and transpiration of fruit trees in Mediterranean areas: a simplified approach. Agric. Meteorol. 171–172, 93–103. https://doi.org/10.1016/j.agrformet.2012.11.010.
Volschenk, T., 2020. Water use and irrigation management of pomegranate trees - a review. Agric. Water Manag. 241, 106375 https://doi.org/10.1016/j.agwat.2020.106375.